

FOSSIL
FUELS
RESEARCH

DOE/BC/10344-15(Vol.2)
(DE85000137)

INVESTIGATIONS OF ENHANCED OIL RECOVERY THROUGH USE
OF CARBON DIOXIDE

Final Report for the Period October 1, 1980—December 31, 1984

Volume II: Displacement Studies

By
Teresa G. Monger

August 1985

By
Louisiana State University
Baton Rouge, Louisiana



National Petroleum Technology Office
U.S. DEPARTMENT OF ENERGY
Tulsa, Oklahoma

DISCLAIMER

This report was prepared as an account of work sponsored by an agency of the United States Government. Neither the United States Government nor any agency thereof, nor any of their employees, makes any warranty, expressed or implied, or assumes any legal liability or responsibility for the accuracy, completeness, or usefulness of any information, apparatus, product, or process disclosed, or represents that its use would not infringe privately owned rights. Reference herein to any specific commercial product, process, or service by trade name, trademark, manufacturer, or otherwise does not necessarily constitute or imply its endorsement, recommendation, or favoring by the United States Government or any agency thereof. The views and opinions of authors expressed herein do not necessarily state or reflect those of the United States Government.

This report has been reproduced directly from the best available copy.

INVESTIGATIONS OF ENHANCED OIL RECOVERY
THROUGH USE OF CARBON DIOXIDE

Final Report for Period
October 1, 1980 - December 31, 1984

Volume II: Displacement Studies

By
Teresa G. Monger, Principal Investigator

and
John H. McMullan, Oscar K. Kimbler, Walter R. Whitehead,
Russell M. Hoshman, Nona S. Sanders, Winton G. Aubert
and Russell Saragusa, Contributors

August 1985

Work Performed Under Contract No. AS19-80BC10344

Fred W. Burtch, Technical Project Officer
Bartlesville Project Office
P.O. Box 1398
Bartlesville, Oklahoma 74005

Prepared for
U.S. Department of Energy
Assistant Secretary for Fossil Energy

Prepared by
Louisiana State University
Department of Petroleum Engineering
Baton Rouge, Louisiana 70803

TABLE OF CONTENTS

	<u>Page</u>
TABLE OF CONTENTS	ii
LIST OF TABLES	iv
LIST OF FIGURES	vi
ABSTRACT	vii
WORK STATEMENT	viii
PART I - SANDPACK DISPLACEMENT STUDIES WITH CARBON DIOXIDE AND BROOKHAVEN RESERVOIR OIL	1
INTRODUCTION	1
EXPERIMENTAL SECTION	4
Samples and Standards	4
Apparatus	8
Time/Temperature Program	8
Preparation of Calibration Curve	8
RESULTS AND DISCUSSION	8
Sample Analyses	8
General Discussion	10
CONCLUSIONS	33
PART II - COREFLOODS USING CARBON DIOXIDE WITH SYNTHETIC OR NATURAL RESERVOIR OIL SYSTEMS	36
INTRODUCTION	36
EXPERIMENTAL SECTION	40
Horizontal Corefloods Using Carbon Dioxide and Synthetic Oil Systems	40
Core Apparatus	40
Synthetic Oils	40
Brine Solutions	43
Pumps and Transfer Vessels	43
Experimental Procedure	43
Compositional Analyses Performed for Corefloods Using Synthetic Oils	47
Samples and Standards	47
Apparatus	48

TABLE OF CONTENTS (continued)

	<u>Page</u>
Time/Temperature Program	48
Samples Analyses	48
Vertical Corefloods Using Carbon Dioxide and Timbalier Bay Reservoir Oil	49
Core Apparatus	49
Timbalier Bay Reservoir Oil	49
Experimental Procedure	49
RESULTS AND DISCUSSION	53
Corefloods Using Synthetic Oils	53
Compositional Analyses Performed For Corefloods Using Synthetic Oils	57
Vertical Coreflood Experimental Results	75
CONCLUSIONS	76
BIBLIOGRAPHY	79

LIST OF TABLES

		<u>Page</u>
1	Compositions of Transition Zone Fluids at 135°F	2
2	GC Analysis of Dead Brookhaven Crude	6
3	Qualitative Compositional Analysis of 5080-8716	7
4	Composition of Brookhaven Crude Oil Samples from SP-49	12
5	Composition of Brookhaven Crude Oil Samples from SP-48	14
6	Composition of Brookhaven Crude Oil Samples from SP-51	16
7	Composition of Brookhaven Crude Oil Samples from SP-47	18
8	Composition of Brookhaven Crude Oil Samples from SP-43	20
9	Composition of Brookhaven Crude Oil Samples from SP-39	22
10	Composition of Brookhaven Crude Oil Samples from SP-46	24
11	Composition of Brookhaven Crude Oil Samples from SP-41	26
12	Composition of Brookhaven Crude Oil Samples from SP-45	28
13	Composition of Brookhaven Crude Oil Samples from SP-33	30
14	Analyses of Effluent from CO ₂ -Brookhaven Oil Sandpack Displacement	34
15	Pore Volumes and Permeability of Berea Sandstone Cores	42
16	Synthetic Oil Compositions	44
17	Synthetic Oil Molecular Structures	45
18	Properties of Synthetic Oils	46
19	Properties of Timbalier Bay Stock Tank Oil	51
20	Results of Unsuccessful Tertiary Core Floods	55
21	Results of Successful Tertiary Core Floods	56
22	Compositional Analyses of Samples from Run 7	58
23	Compositional Analyses of Samples from Run 9	60
24	Compositional Analyses of Samples from Run 4	62
25	Compositional Analyses of Samples from Run 8	64

LIST OF TABLES (Continued)

	<u>Page</u>
26 Compositional Analyses of Samples from Run 5	66
27 Compositional Analyses of Samples from Run 6	68
28 Compositional Analyses of Samples from Run 1	70
29 Compositional Analyses of Samples from Run 2	71
30 Compositional Analyses of Samples from Run 3	72
31 Compositional Profile of Synthetic Oils Without C ₅	74
32 Results of Vertical Corefloods	77
33 Phase Behavior Observations During Vertical Corefloods	78

LIST OF FIGURES

		<u>Page</u>
1	Ultimate Recovery from Sand Pack Displacements of Dead Brookhaven Curve Oil	5
2	Calibration Curve of Standard 5080-8716	9
3	Typical Crude Oil Chromatogram	11
4	Composition of Brookhaven Crude Oil Samples from SP-49	13
5	Composition of Brookhaven Crude Oil Samples from SP-48	15
6	Composition of Brookhaven Crude Oil Samples from SP-51	17
7	Composition of Brookhaven Crude Oil Samples from SP-47	19
8	Composition of Brookhaven Crude Oil Samples from SP-43	21
9	Composition of Brookhaven Crude Oil Samples from SP-39	23
10	Composition of Brookhaven Crude Oil Samples from SP-46	25
11	Composition of Brookhaven Crude Oil Samples from SP-41	27
12	Composition of Brookhaven Crude Oil Samples from SP-45	29
13	Composition of Brookhaven Crude Oil Samples from SP-33	31
14	Pressure-Composition (P-X) Diagram of Oil P/A	37
15	Pressure-Composition (P-X) Diagram of Oil P	38
16	Pressure-Composition (P-X) Diagram of Oil P/A-P	39
17	Schematic of Horizontal Coreflood Apparatus	41
18	Schematic of Vertical Coreflood Apparatus	50
19	Compositional Analyses of Samples from Run 7	59
20	Compositional Analyses of Samples from Run 9	61
21	Compositional Analyses of Samples from Run 4	63
22	Compositional Analyses of Samples from Run 8	65
23	Compositional Analyses of Samples from Run 5	67
24	Compositional Analyses of Samples from Run 6	69

ABSTRACT

The lowest pressure at which CO₂ can develop miscibility with a particular reservoir oil is termed the "minimum miscibility pressure" (MMP). There are two major factors which determine the CO₂ MMP, reservoir temperature and crude oil composition. While sufficient evidence exists indicating that oil composition affects the CO₂ MMP, the magnitude of this effect and the importance of hydrocarbon chemistry are not clearly defined.

The purpose of this investigation was to use compositional data to suggest how the compositional changes which accompany a CO₂ oil displacement affect the observed recovery efficiency. The experimental approach was to perform sandpack displacements of dead Brookhaven crude oil at a variety of temperatures and pressures (Part I), and to perform corefloods using CO₂ with synthetic or natural reservoir oil systems (Part II).

The sandpack results provide compositional proof that for a given temperature, increasing pressure affects greater oil recovery. Compositional analyses of samples from displacements performed at lower pressures indicate that the major components extracted into the CO₂-rich phase are in the C₉ - C₁₂ range. As the run pressure is increased, the ability of CO₂ to extract heavier hydrocarbons improves to provide greater oil recoveries.

Several reports in the literature suggest that oil aromaticity affects the process by which CO₂ displaces reservoir oil, in a manner which augments other oil compositional effects. Phase compositional analyses performed for CO₂-synthetic oil mixtures which model the phase behavior of CO₂-crude oil systems, have demonstrated that increased oil aromaticity correlates with improved hydrocarbon extraction into a CO₂-rich phase. To determine whether the improvement in hydrocarbon extraction observed in static PVT measurements would translate into higher oil recoveries in CO₂ displacement tests, tertiary corefloods were performed using the synthetic oils. The coreflood results show that the oil displacement efficiency for CO₂ flooding is improved by increasing the aromatic content of the oil. These influences of oil aromaticity are favorable.

Another series of corefloods was initiated to examine the gravity stable displacement process. As far as implementation of a gravity stable, multiple-contact miscible CO₂ flood is concerned, recent field tests are providing encouraging results from a technical standpoint. From an economical standpoint, however, the benefits of improved oil recovery are threatened by the long lead times imposed by gravity stable injection rates. Ongoing experiments are quantitating the incremental oil recovered with injection rate reduction for a reservoir amenable to gravity stable flooding. Progress to date is presented.

WORK STATEMENT

The contract with the U.S. Department of Energy required the performance of five tasks. Two of these tasks relate to phase behavior studies and are addressed in Volume I of this final report. The remaining three tasks relate to displacement studies as summarized below:

TASK I

To extend the study of multiple contact miscibility mechanism(s) associated with carbon dioxide and crude oil using slim-tube displacements.

- (a) Displacement studies using live Brookhaven crude oil will be made to determine the minimum miscibility pressure over a range of temperatures.
- (b) Samples taken at run temperature and pressure during the live Brookhaven displacements will be analyzed using gas chromatographs. The compositional paths will be studied in an attempt to identify the displacement mechanism(s).
- (c) Displacements using dead Brookhaven crude oil will be made over a range of temperatures and pressures to investigate the role of lower molecular weight hydrocarbons on minimum miscibility pressure.
- (d) Analysis of samples taken during the dead oil displacements will be analyzed using gas chromatographic techniques to allow comparison of compositional paths to the live oil displacements.

TASK II

To extend the study of multiple-contact miscibility mechanism(s) associated with carbon dioxide and crude oil using displacements in consolidated cores.

- (a) Apparatus will be assembled to allow gravity stable displacements at reservoir temperature and pressure in consolidated Berea sandstone cores.
- (b) A series of displacements performed in these consolidated cores will be made using crude oil, and synthetic oils composed of selected paraffinic and aromatic hydrocarbons to illuminate the relationship(s) between displacement efficiency and the phase behavior studies summarized in Task III. The effects of water saturation will be studied for selected fluid systems.

TASK V

To study the plugging of consolidated cores observed when Brookhaven crude is displaced by carbon dioxide.

- (a) The effects of temperature and pressure on the formation of the plugging material will be investigated.
- (b) The role of miscibility in the generation of the plugging material will be examined.

- (c) Chemical tests will be performed in an attempt to identify the composition of the plugging material.

Full details of these completed contract requirements are presented in Volume II of this final report with three exceptions: (1) work performed in support of subtask Ia has been previously reported (Whitehead et al., 1981), (2) work performed in support of subtask Ib has been previously reported (Whitehead et al., 1981; Monger, 1985), and (3) work performed in support of subtask Ic has been previously reported (Monger and McMullan, 1983).

PART I - SANDPACK DISPLACEMENT STUDIES WITH CARBON
DIOXIDE AND BROOKHAVEN RESERVOIR OIL

INTRODUCTION

Several mechanisms have been proposed to describe miscibility development in the multiple-contact miscible CO₂ flooding process (Stalkup, 1983). Reservoir temperature and pressure are certainly important factors in determining which mechanism predominates. The composition of the reservoir oil is perhaps equally significant because of the effects of oil composition on CO₂-crude oil phase behavior.

Oil compositional effects in CO₂ flooding have been addressed by many investigators using a variety of largely experimental approaches. In a study examining miscible phase or solvent flooding processes involving CO₂, Holm (1959) stated that oil recovery is a function of the mutual solubility of reservoir oil and CO₂. Preliminary solubility determinations of CO₂ in hydrocarbons at 125°F indicated that in addition to pressure, the solubility varied with molecular weight and type of hydrocarbon. Rathmell et al. (1971) conducted CO₂ displacements of reconstituted reservoir fluids in Boise outcrop sandstone cores, ranging in length from 6 to 42.5 ft. They reported that CO₂ miscibility is generated through multiple-contact equilibria in which the CO₂ is progressively enriched with hydrocarbon components in the C₂ to C₆ range from the oil. Their results also indicated that increasing the methane content in the reservoir fluid serves to increase the miscibility pressure. Holm and Josendal (1974) conducted miscible CO₂ displacements of Mead-Strawn stock-tank oil and Bandini stock-tank oil in 48 ft. sandpacks. Compositional analyses of transition zone fluids indicated that the components extracted during the floods were primarily middle range (C₇ to C₃₀) hydrocarbons with few heavy (C₃₀+) or light ends (<C₇) (Table 1). In addition, displacements of Bandini stock-tank oil exhibited earlier and more extensive extraction of lighter hydrocarbons at lower pressures. Compositional analyses of the Bandini crude indicated a larger amount of hydrocarbons in the gasoline and light gas-oil range, thus illustrating the importance of reservoir fluid composition on the development of miscibility. Holm and Josendal (1974) also reported that the presence of methane in the injection fluid increases the optimum displacement pressure; while, the presence of methane in the reservoir oil does not appreciably change the optimum displacement pressure, but serves to reduce the overall recovery efficiency. Metcalfe and Yarbrough (1979) proposed that the mechanism of miscibility development is directly related to the phase equilibria of a CO₂/reservoir-fluid system. Displacement mechanisms were examined by experimentally determining the compositional changes which occurred between CO₂ and several synthetic oils during corefloods performed at varying temperatures and pressures. They claimed that a vaporization mechanism predominates at high temperatures and pressures; while, at equivalent pressures and lower temperatures, the mechanism is described as a condensation of CO₂ into an oil-rich phase, typical of liquid-liquid equilibria. Leach and Yellig (1979) conducted experimental displacements of a ten component synthetic oil (C₁-C₁₄) in sandstone cores at a variety of temperatures and pressures. Compositional profiles obtained for each displacement indicated that the primary mechanism is a condensation type process, as previously observed in rich gas displacements. The synthetic oil studied, however, is

Table 1

(after Holm and Josendal, 1974)

Compositions of Transition Zone Fluids at 135°F (mole %)					
Hydrocarbon Boiling Range °F	Estimated Carbon Number	Mead-Strawn Stock-Tank Oil	Extracted During 2,500 psig Flood	Extracted During 2,200 psig Flood	Extracted During 1,800 psig Flood
To 170	C ₃ to C ₆	16.9	2.1	2.5	1.6
175 to 850	C ₁ to C ₃₀	79.2	96.3	96.5	97.7
> 850	C ₄₃	<u>3.9</u>	<u>1.6</u>	<u>1.0</u>	<u>0.7</u>
		100.0	100.0	100.0	100.0

not representative of any reservoir oil in that it is composed of strictly paraffinic hydrocarbons, the heaviest component of which is C_{14} . Huang and Tracht (1974) conducted tertiary displacements of a 36° API West Texas oil in Berea sandstone cores at reservoir conditions of 90°F and 1250 psig. Phase behavior studies of the CO_2 /crude oil system were also performed in order to examine the effects of temperature and pressure on the phase equilibria. A liquid-liquid equilibrium phenomenon was observed at 90°F and elevated pressures when the CO_2 /crude oil mixture contained greater than 75 mole per cent CO_2 . The CO_2 -rich liquid phase was found to contain approximately 12 mole per cent hydrocarbons. They concluded that CO_2 swelling and extraction are the dominant mechanisms involved in the recovery of residual oil. Gardner et al. (1981) performed slim-tube displacements with CO_2 and Wasson crude oil at 1350 and 2000 psia. Single-contact and multiple-contact PVT experiments were also performed in an attempt to establish the relationships between phase behavior and displacement efficiency. Compositional data obtained from the single- and multiple-contact experiments indicated the preferential accumulation of lighter components in the upper phases; while, the heavier components tended to concentrate in the lower phases. From these results, Gardner et al. (1981) described the displacement mechanisms at both pressures as a vaporizing gas drive. Orr et al. (1981) examined the complex phase behavior of CO_2 /crude oil systems in low temperature reservoirs to determine the influence of liquid-liquid and liquid-liquid-vapor phase behavior on the displacement mechanism. Single-contact phase equilibria results indicated that liquid-liquid phase behavior can be expected for crude oils at temperatures below 50°C (122°F) and that displacements of oil by CO_2 develop miscibility by the extraction of hydrocarbon components into a CO_2 -rich phase when this phenomenon occurs. In a more recent study, Orr et al. (1982) performed continuous multiple-contact displacements of Maljamar separator oil at 90°F (32°C) and four pressures: 800, 1000, 1200, and 1400 psia. Compositional analyses and density measurements demonstrated that a CO_2 -rich liquid phase can contain as much as 20-30 weight per cent hydrocarbons and that a CO_2 -rich vapor phase at the same conditions extracts hydrocarbons less efficiently. Slim-tube displacements indicated increased oil recoveries when displacement pressures were high enough to affect the liquid-liquid phase behavior, likewise indicating the improved extraction efficiency of the CO_2 -rich liquid phase.

Holm and Josendal (1980) conducted an extensive study into the effects of oil composition on miscible CO_2 displacements in order to confirm a previous correlation relating oil composition and MMP. According to Holm and Josendal (1980), CO_2 extracts hydrocarbons from the reservoir oil until a sufficient quantity of these components exists at the flood front for a miscible displacement to occur. Results of slim-tube displacements performed on a wide variety of crude oils indicated that maximum oil recovery and the pressure required to achieve it are functions of the amount of C_5 to C_{30} components and the distribution of these components in the crude oil. Furthermore, attempting to demonstrate the effect of oil type (paraffin/aromatic), slim-tube displacements with a highly paraffinic oil and a hybrid oil were compared. The hybrid oil was comprised of the paraffinic oil with its higher boiling fraction replaced by more aromatic material. The results of these displacements indicated that oil recovery was greater for the more aromatic oil. Monger and Khakoo (1981) examined the phase behavior of CO_2 with two Appalachian crude oils at temperatures above and below the CO_2 critical temperature. Several aspects of the CO_2 /Appalachian crude phase behavior contrast with that reported for the CO_2 /Western crude oil systems. These differ-

ences were attributed to the lower aromatic content of the Appalachian crudes. Further data analyses suggested that CO₂ preferentially condenses into a highly paraffinic oil; whereas, hydrocarbon extraction by a CO₂-rich phase is the predominant mechanism encountered for crude oils having considerable aromatic content. Based on visual observations, swelling indices, and comparative phase behavior analyses, Monger and Khakoo (1981) hypothesized that increasing crude oil aromaticity correlates with improved hydrocarbon extraction into a CO₂-rich phase.

EXPERIMENTAL SECTION

The Brookhaven crude oil samples analyzed were obtained from previously reported sandpack displacements performed under Task Ic (Monger and McMullan, 1983) The results of these displacements are summarized in Figure 1. The MMP is interpreted as being the pressure at which the first break in the recovery versus pressure curve occurs. The rapid increase in recovery occurring at pressures beyond the MMP in the curves at 140°F and 175°F is believed to be related to the high asphaltic content of Brookhaven crude.

The compositional analyses of these samples were performed using gas chromatography in accordance with ASTM Method D2887-73 (ASTM Book of Standards, Method D2887-73, American Society for Testing and Materials, 1916 Race Street, Philadelphia, PA 19103). According to this procedure, mixtures of hydrocarbons with boiling points ranging through approximately 1000°F (528°C) can be determined by, first, constructing a calibration curve of boiling point versus retention time for a qualitative standard, consisting of various hydrocarbons through C₄₀. This enables the assignment of retention times to the various hydrocarbon components in order to qualitatively characterize subsequent crude oil samples. Under identical temperature conditions, a sample is then introduced into the chromatographic column which is capable of separating the hydrocarbons in boiling point order within a limited range. The column temperature is increased at some prescribed rate, and the area under the chromatogram is recorded throughout the run. ASTM Method D2887-73 does not consider response factors for the C₅ - C₄₀ components; therefore, the area percent associated with a particular hydrocarbon approximates the weight per cent of that component in this range.

Samples and Standards

The compositional analysis of virgin Brookhaven crude oil is presented in Table 2. Samples of sandpack effluent were flashed to ambient conditions at various points during each displacement. The dead oil samples were placed in airtight glass vials and refrigerated. Prior to gas chromatographic analyses, the samples were allowed to warm to room temperature for approximately one hour in order to obtain a well-mixed, liquid sample for injection.

The qualitative, standard calibration mixture (5080 - 8716) was obtained from Hewlett Packard, and its composition is presented in Table 3. Gentle warming of this standard before use was necessary to redissolve the heavier components, which precipitated upon standing at room temperature.

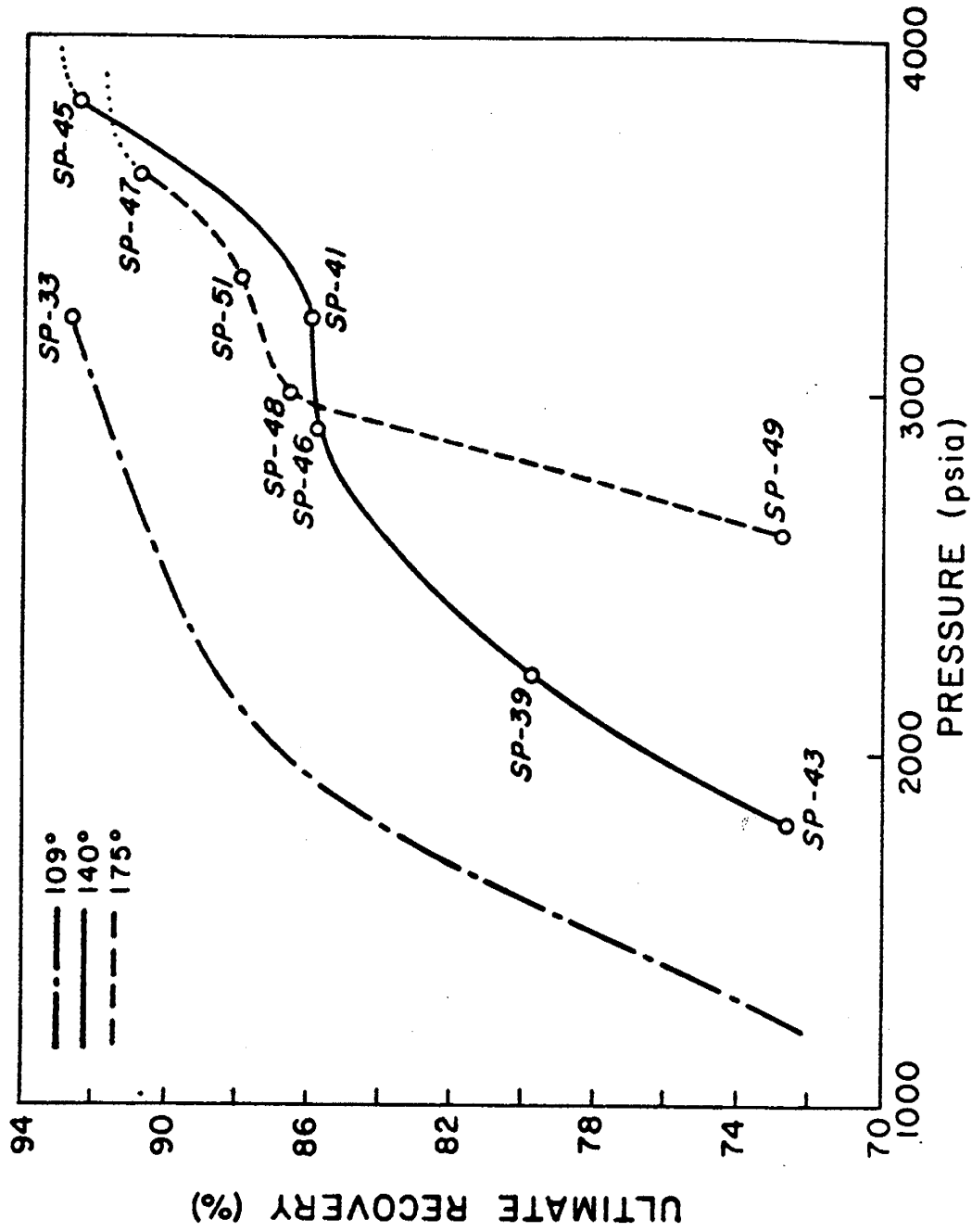


Figure 1. Ultimate Recovery from Sand Pack Displacements of Dead Brookhaven Crude Oil

Table 2
GC Analysis of Dead Brookhaven Crude

<u>Component</u>	<u>Mole Per Cent</u>
C ₁	0.46
C ₂	1.0
C ₃	0.23
C ₄	2.8
C ₅	1.1
C ₆	2.8
C ₇	7.0
C ₈	4.5
C ₉ , C ₁₀	11.6
C ₁₁ , C ₁₂	13.1
C ₁₃ , C ₁₄	12.1
C ₁₅ , C ₁₆	11.9
C ₁₇ , C ₁₈	12.1
C ₁₉ , C ₂₀ , C ₂₁	9.2
C ₂₂ , C ₂₃ , C ₂₄ , C ₂₅	6.5
C ₂₆ , C ₂₇ , C ₂₇	0.9
C ₃₁	0.1
C ₃₂	0.1

Table 3

Qualitative Compositional Analysis of 5080 - 8716

<u>Component</u>	<u>Boiling Point (°C)</u>
C ₅	36
C ₆	69
C ₇	98
C ₈	126
C ₉	151
C ₁₀	174
C ₁₁	196
C ₁₂	216
C ₁₄	253
C ₁₅	271
C ₁₆	287
C ₁₇	302
C ₁₈	317
C ₂₀	344
C ₂₄	391
C ₂₈	423
C ₃₂	468
C ₃₆	498
C ₄₀	525

Apparatus

The compositional analyses were performed using the Hewlett Packard 5880 gas chromatograph equipped with two thermal conductivity detectors (TCD). The columns consisted of 6 foot long, $\frac{1}{8}$ inch outside diameter Nickel-200 columns packed with 10 per cent OV 101 on Chromosorb W. These columns were conditioned by heating them from 0°C to 340°C at a rate of 10°C/minute with no carrier gas flowing. When the oven temperature reached 340°C, the flow of carrier gas was resumed, and the columns were allowed to bake at this temperature for 48 hours. At no time during the conditioning procedure were the columns connected to the detectors. The carrier gas used was 99.995 per cent pure Helium gas equipped with a moisture trap, and carrier gas flow rates were adjusted to 40 cc/minute \pm 0.5 cc. Injections were made with a 10 microliter Hamilton gas-tight syringe.

Time/Temperature Program

The time/temperature program employed in the analysis of the dead crude oil samples is presented below.

Oven Temperature Profile:

Initial Value	=	30°C
Initial Time	=	3.00 minutes
Program Rate	=	10°C/minute
Final Value	=	340°C
Final Time	=	20.00 minutes

The injection port temperatures were set at 300°C, while the detector temperatures were set at 370°C. These temperatures were maintained as such to prevent the build-up of carbon residue in these portions of the instrument. In addition the columns were allowed to bake overnight at 340°C throughout the testing period in an effort to minimize residual sample contamination.

Preparation of Calibration Curve

The calibration curve was prepared by injecting 1 microliter of the standard, 5080 - 8716, into the 5880, which was programmed according to the previously listed time and temperature parameters. From the resulting chromatogram, a plot of boiling point versus retention time was constructed (Figure 2). This calibration curve was used to identify components in the following sample analyses.

RESULTS AND DISCUSSION

Sample Analyses

Upon standing at room temperature for one hour, the samples were shaken to ensure adequate mixing, then one microliter samples were analyzed under the

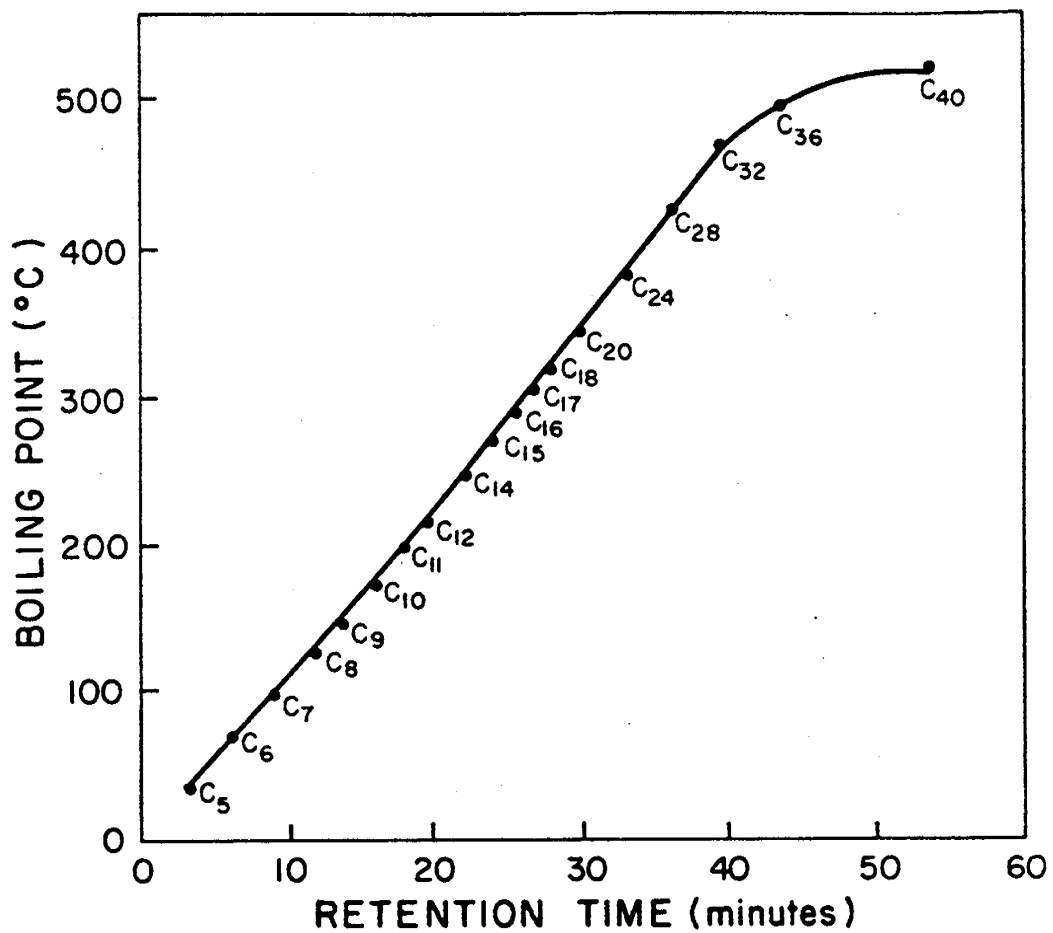


Figure 2. Calibration Curve of Standard 5080-8716

exact time/temperature conditions as the standard. Because crude oil is composed of such numerous hydrocarbon components and associated isomers, it is impossible to identify or quantitate individual peaks (Figure 3). The "time slice" method (Hewlett Packard 5880A Gas Chromatograph Manual, Integration and Methods, Vol. 5, August, 1979) was, therefore, used to integrate the area under the crude oil chromatograms. Incremental chromatographic areas were recorded at 0.2 minute (12 seconds) intervals, which facilitated the summing of area counts based on component retention times specified by the calibration curve. Assuming that the area per cent was equivalent to the weight per cent of a particular component, the percentages were then converted to mole fractions.

The results of these analyses are presented in tabular form in Tables 4 through 13 and graphically in Figures 4 through 13. In addition to the compositional analyses, visual observations recorded during the displacements at the time of sampling are also presented. Sampling times are reported using a dimensionless variable referred to as the fractional run time (FRT).

$$FRT = \frac{\text{cc's of CO}_2 \text{ injected at the time of sampling}}{\text{cc's of CO}_2 \text{ injected at GOR} = 30,000 \text{ SCF/STB}}$$

The cc's of CO₂ injected were measured at room temperature and run pressure.

General Discussion

Samples procured in the early stages of the displacements are representative of the virgin oil, while samples obtained just prior to the appearance of two phases represent a combination of the in place oil and the miscible displacing fluid. Samples collected later in the displacements, particularly during the flow of two phases are considered to be transition zone fluids. The profiles observed in the transition zone are especially significant in that these samples indicate the extent of hydrocarbon extraction, which occurs in the development of miscibility. This phenomenon is directly related to the recovery efficiency of the process.

According to the compositional analyses of samples from SP-49 (T = 175°F, P = 2600 psia), a slight increase is observed in the C₅ - C₈ range. An appreciable increase is noted in the C₉ - C₁₂ fraction, with decreases occurring in the C₁₃ - C₃₂ range. The ultimate recovery from this run was 73.0%. The compositional profile of transition zone fluids procured during the displacement of Brookhaven crude oil at the CO₂ MMP, SP-48 (T = 175°F, P = 3000 psia), indicates decreases in all fractions except the C₉ - C₁₂ fraction, which increases significantly. The ultimate recovery from this displacement was 87.1%. Analyses of samples obtained from SP-51 (T = 175°F, P = 3300 psia), indicate that a slight increase is observed in the C₅ - C₈ fraction; while a significant increase is noted in the C₉ - C₁₂ range. Decreases were observed in all other hydrocarbon fractions. The recovery obtained from this displacement was 88.1%.

It appears that the most significant extraction of hydrocarbons into the CO₂-rich phase of the transition zone occurred in the C₉ - C₁₂ range for the aforementioned displacements. Variations in the C₅ - C₈ fraction fluctuate

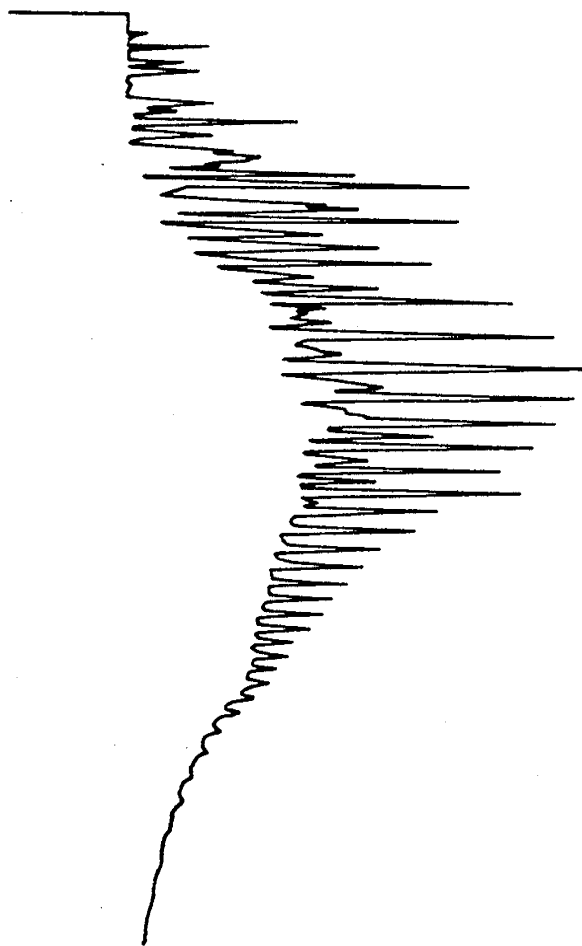


Figure 3. Typical Crude Oil Chromatogram

Table 4

Composition of Brookhaven Crude Oil Samples from SP-49
(mole fractions)

SP-49

P = 2600 psia

% Recovery: 73.0%

T = 175°F

Sample No.	1	2	3
Observation	Black; Single Phase	Black; Single Phase	Brown and Clear Phase; Two Phase
FRT	0.30	0.68	0.82
Components			
C ₅ - C ₈	0.25	0.25	0.26
C ₉ - C ₁₂	0.29	0.30	0.35
C ₁₃ - C ₁₆	0.20	0.19	0.19
C ₁₇ - C ₂₀	0.12	0.12	0.10
C ₂₁ - C ₂₄	0.07	0.07	0.05
C ₂₅ - C ₂₈	0.04	0.04	0.03
C ₂₉ - C ₃₂	<u>0.03</u>	<u>0.03</u>	<u>0.02</u>
	1.00	1.00	1.00

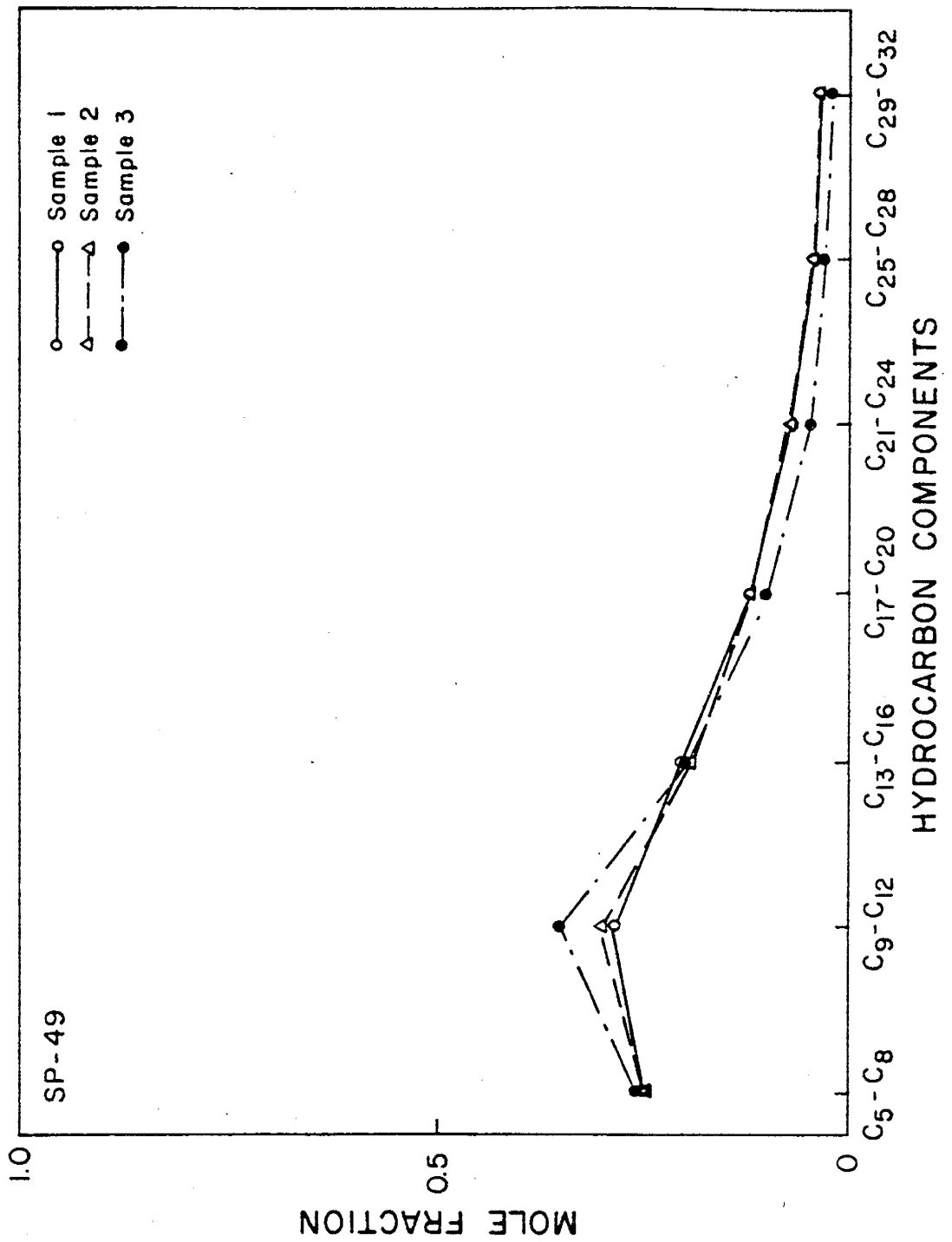


Figure 4. Composition of Brookhaven Crude Oil Samples from SP-49
 (P = 2,600, T = 175°F)

Table 5

Composition of Brookhaven Crude Oil Samples from SP-48
(mole fractions)

SP-48

P = 3000 psia

% Recovery: 87.1%

T = 175°F

Sample No.	1	2	3
Observations	Black; Single Phase	Black; Single Phase	Clear; Single Phase
FRT	0.27	0.65	0.75
Components			
C ₅ - C ₈	0.26	0.24	0.22
C ₉ - C ₁₂	0.27	0.30	0.38
C ₁₃ - C ₁₆	0.21	0.21	0.20
C ₁₇ - C ₂₀	0.12	0.12	0.10
C ₂₁ - C ₂₄	0.07	0.06	0.05
C ₂₅ - C ₂₈	0.04	0.04	0.03
C ₂₉ - C ₃₂	<u>0.03</u>	<u>0.03</u>	<u>0.02</u>
	1.00	1.00	1.00

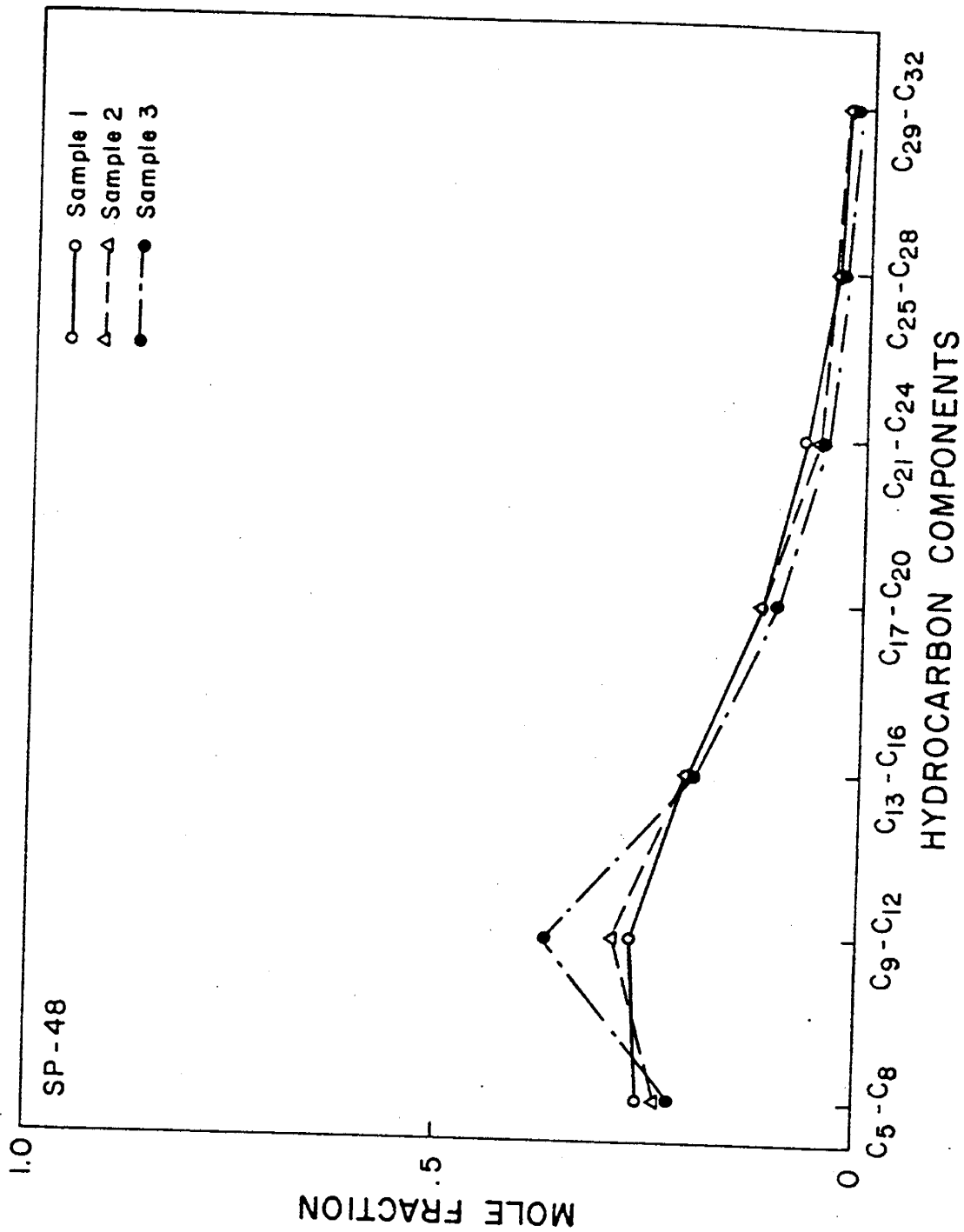


Figure 5. Composition of Brookhaven Crude Oil Samples from SP-48
 (P = 3,000 psia, T = 175°F)

Table 6

Composition of Brookhaven Crude Oil Samples from SP-51
(mole fractions)

SP-51

P = 3300 psia

% Recovery: 88.1%

T = 175°F

Sample No.	1	2	3
Observations	Black; Single Phase	Black; Single Phase	Clear; Single Phase
FRT	0.23	0.60	0.76
Components			
C ₅ - C ₈	0.25	0.25	0.26
C ₉ - C ₁₂	0.26	0.32	0.33
C ₁₃ - C ₁₆	0.22	0.18	0.20
C ₁₇ - C ₂₀	0.13	0.12	0.11
C ₂₁ - C ₂₄	0.07	0.07	0.05
C ₂₅ - C ₂₈	0.04	0.04	0.03
C ₂₉ - C ₃₂	<u>0.03</u>	<u>0.02</u>	<u>0.02</u>
	1.00	1.00	1.00

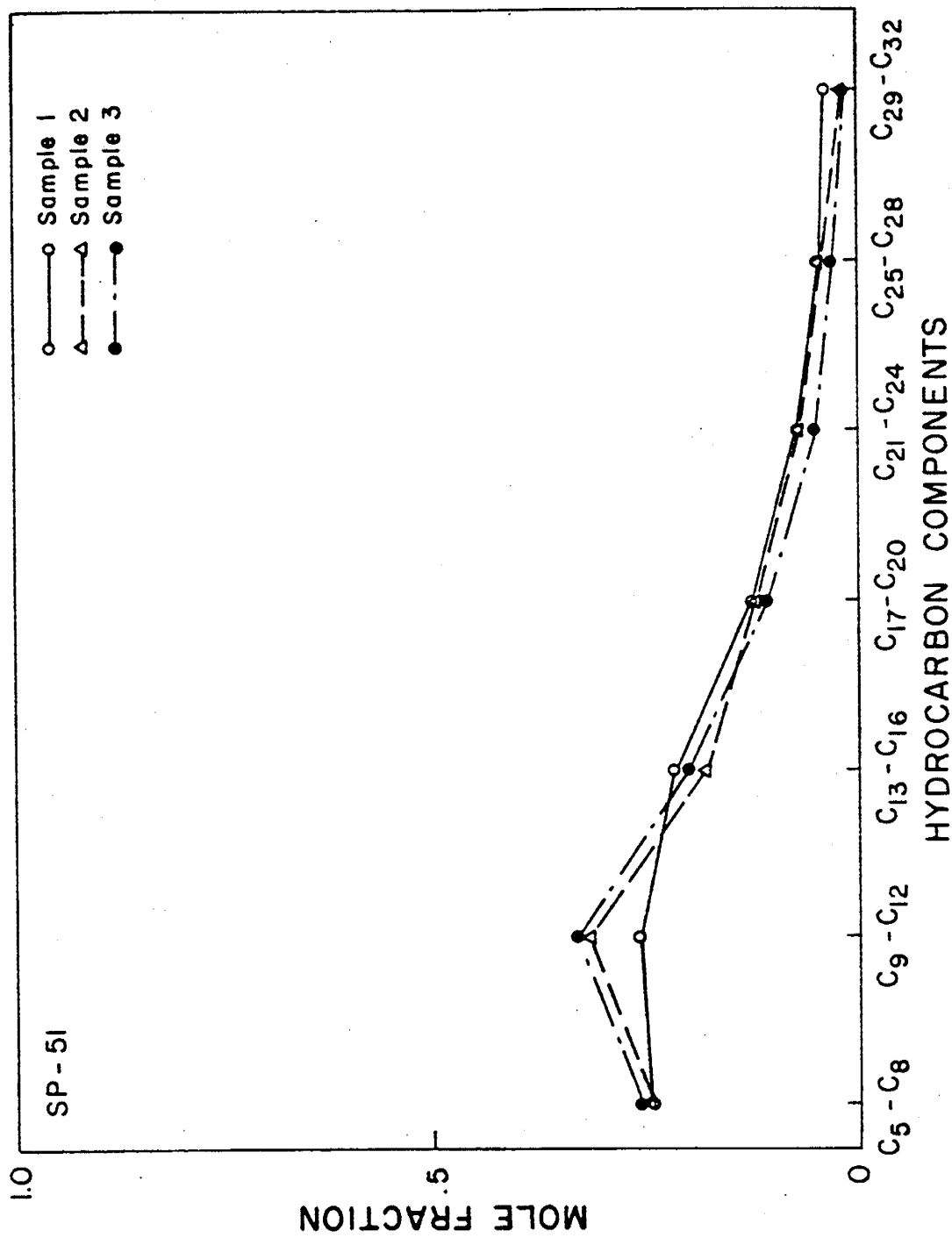


Figure 6. Composition of Brookhaven Crude Oil Samples from SP-51
 (P = 3,300 psia, T = 175°F)

Table 7

Composition of Brookhaven Crude Oil Samples from SP-47
(mole fractions)

SP-47

P = 3600 psia

% Recovery: 91.1%

T = 175°F

Sample No.	1	2	3	4
Observations	Black; Single Phase	Black and Brown Phases; Two Phase	Black; Single Phase	Clear; Single Phase
FRT	0.29	0.77	0.88	0.98
Components				
C ₅ - C ₈	0.28	0.16	0.21	0.17
C ₉ - C ₁₂	0.22	0.32	0.35	0.40
C ₁₃ - C ₁₆	0.22	0.24	0.20	0.23
C ₁₇ - C ₂₀	0.13	0.14	0.12	0.11
C ₂₁ - C ₂₄	0.07	0.07	0.06	0.05
C ₂₅ - C ₂₈	0.05	0.04	0.04	0.03
C ₂₉ - C ₃₂	<u>0.03</u>	<u>0.03</u>	<u>0.02</u>	<u>0.01</u>
	1.00	1.00	1.00	1.00

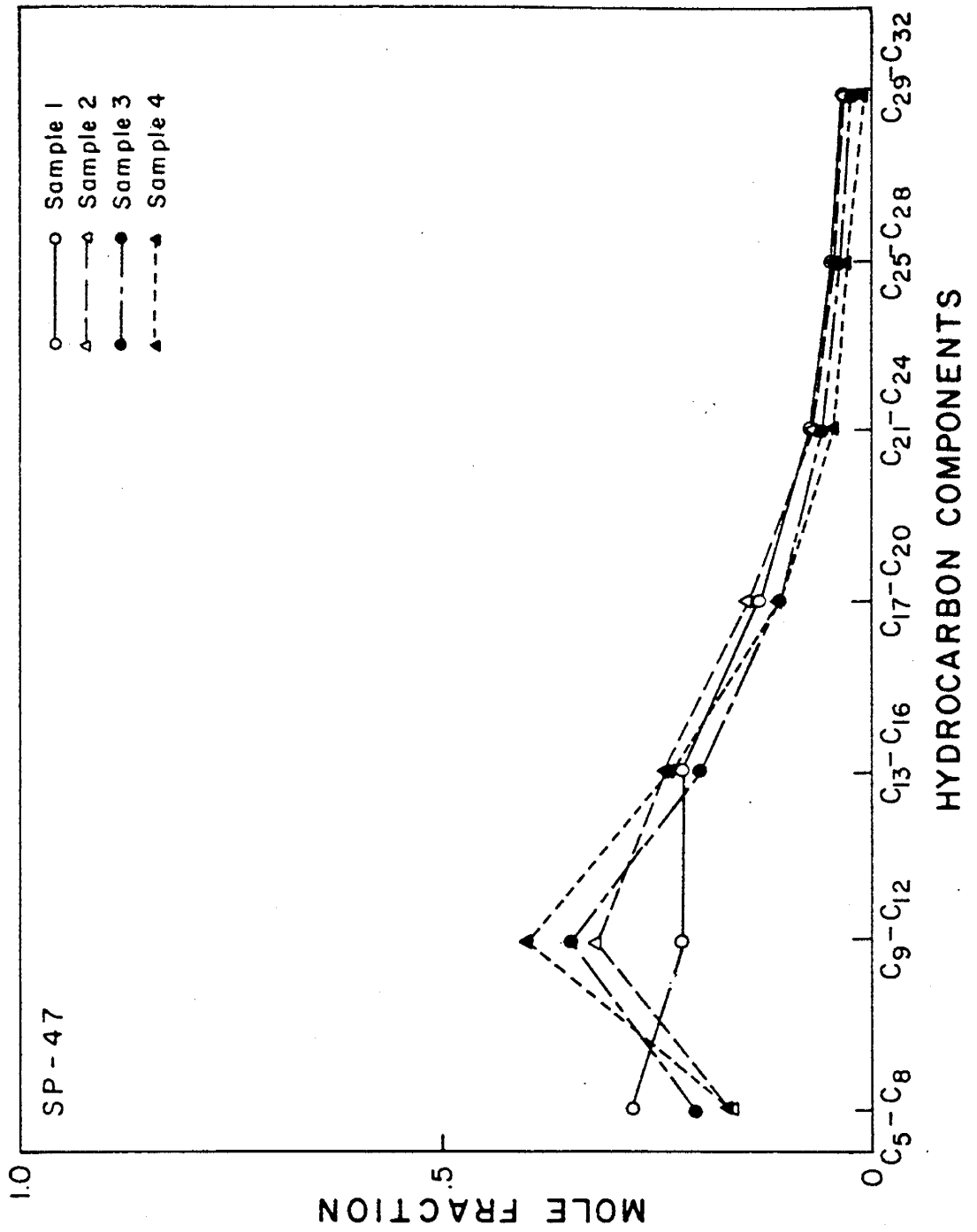


Figure 7. Composition of Brookhaven Crude Oil Samples from SP-47 (P = 3,600 psia, T = 175°F)

Table 8

Composition of Brookhaven Crude Oil Samples from SP-43
(mole fractions)

SP-43

P = 1800 psia

% Recovery: 72.8%

T = 140°F

Sample No.	1	2	3
Observations	Black; Single Phase	Brown and Black Phases; Two Phase	Brown and Black Phases; Two Phase
FRT	0.33	0.79	1.00
Components			
C ₅ - C ₈	0.25	0.24	0.17
C ₉ - C ₁₂	0.29	0.20	0.42
C ₁₃ - C ₁₆	0.19	0.20	0.21
C ₁₇ - C ₂₀	0.12	0.11	0.10
C ₂₁ - C ₂₄	0.07	0.06	0.05
C ₂₅ - C ₂₈	0.04	0.03	0.03
C ₂₉ - C ₃₂	<u>0.04</u>	<u>0.03</u>	<u>0.02</u>
	1.00	1.00	1.00

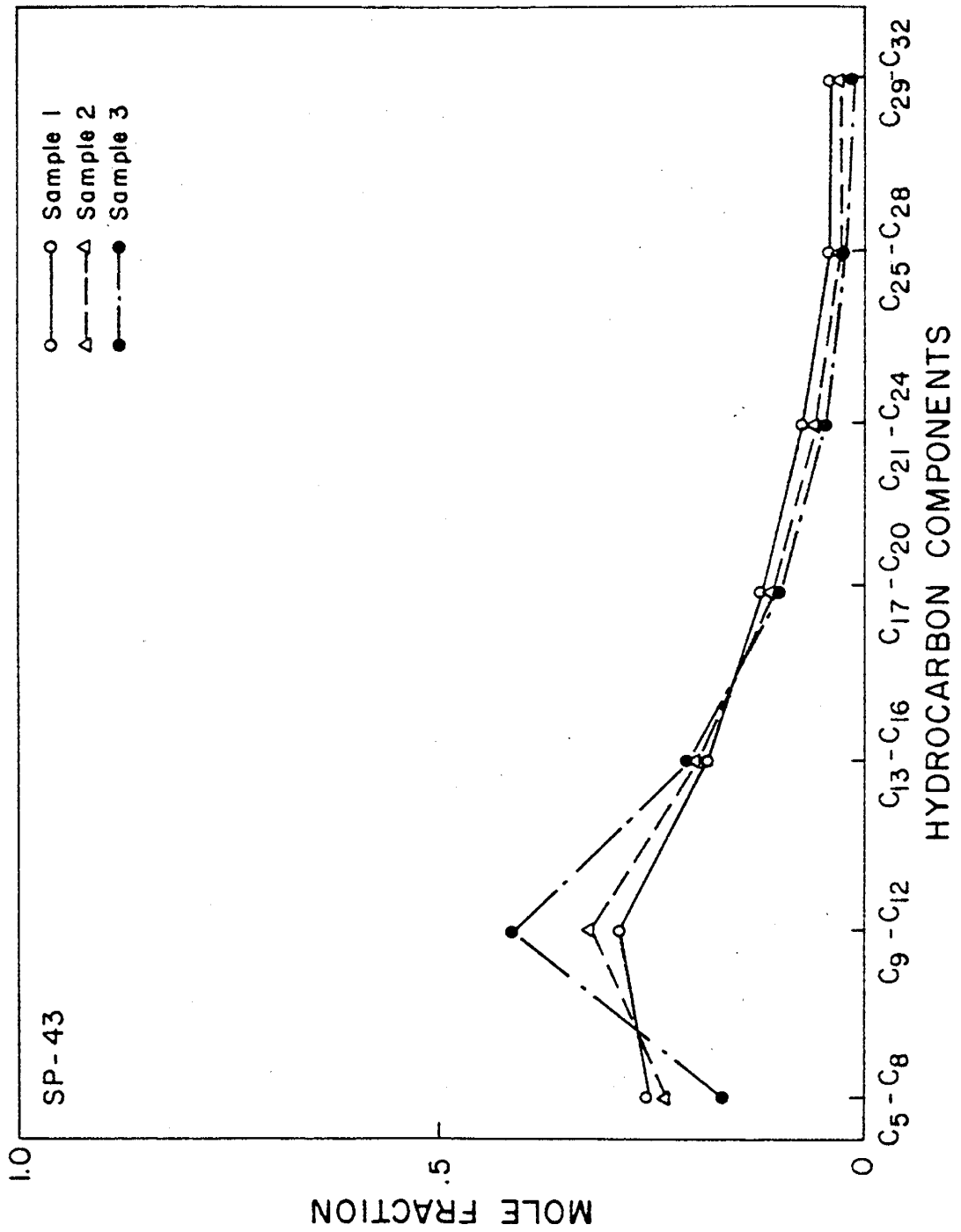


Figure 8. Composition of Brookhaven Crude Oil Samples from SP-43
 (P = 1,800 psia, T = 140°F)

Table 9

Composition of Brookhaven Crude Oil Samples from SP-39
(mole fractions)

SP-39

P = 2200 psia

% Recovery: 79.6%

T = 140°F

Sample No.	1	2	3	4
Observations	Black; Single Phase	Black; Two Phase	Brown; Two Phase	Light Brown; Two Phase
FRT	0.29	0.60	0.72	0.85
Components				
C ₅ - C ₈	0.23	0.29	0.31	0.17
C ₉ - C ₁₂	0.29	0.28	0.39	0.49
C ₁₃ - C ₁₆	0.21	0.18	0.17	0.22
C ₁₇ - C ₂₀	0.12	0.11	0.08	0.07
C ₂₁ - C ₂₄	0.07	0.07	0.03	0.03
C ₂₅ - C ₂₈	0.04	0.04	0.01	0.01
C ₂₉ - C ₃₂	<u>0.04</u>	<u>0.03</u>	<u>0.01</u>	<u>0.01</u>
	1.00	1.00	1.00	1.00

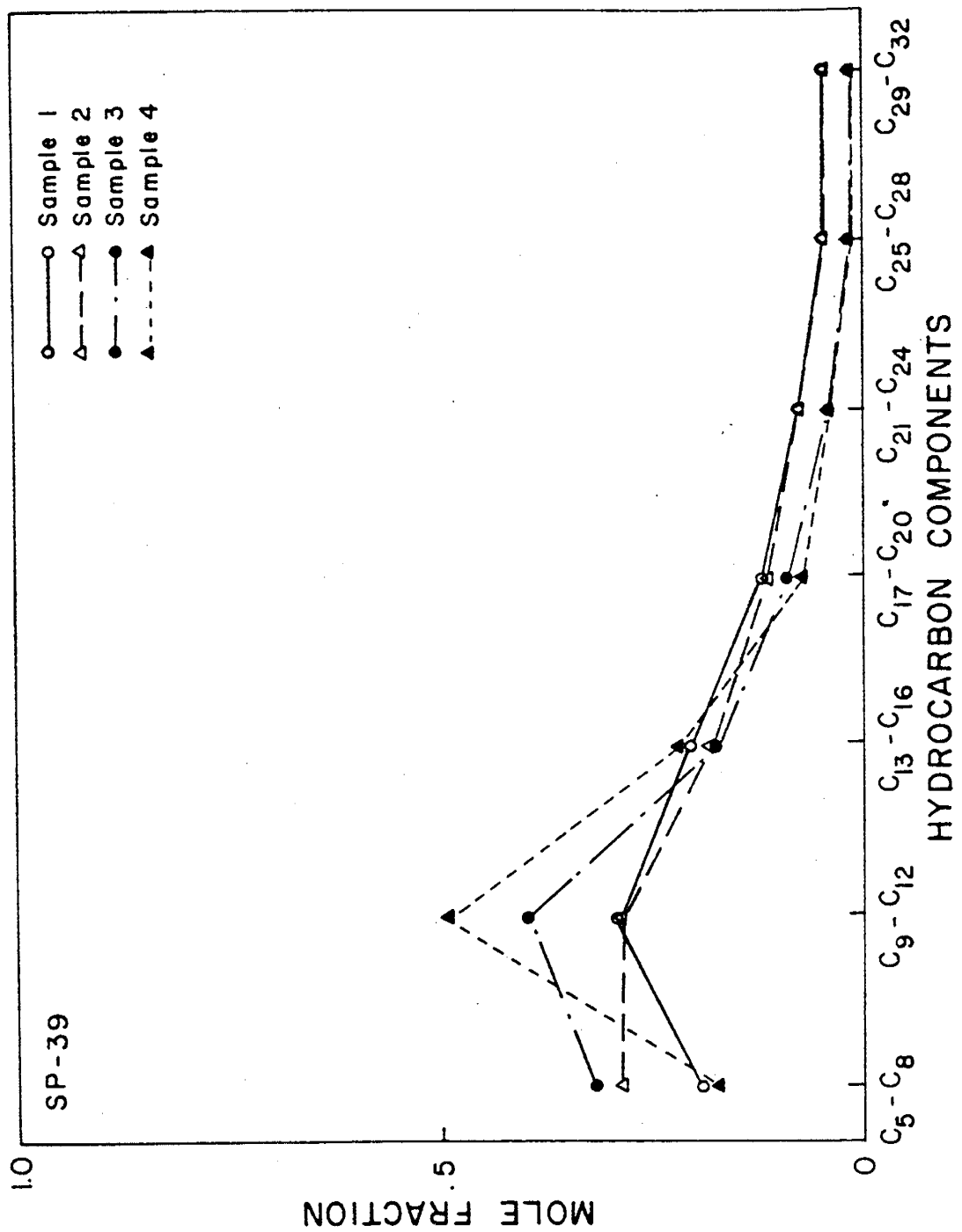


Figure 9. Composition of Brookhaven Crude Oil Samples from SP-39
(P = 2,200 psia, T = 140°F)

Table 10

Composition of Brookhaven Crude Oil Samples from SP-46
(mole fractions)

SP-46

P = 2900 psia

% Recovery: 86.1%

T = 140°F

Sample No.	1	2	3	4
Observations	Black; Single Phase	Black; Single Phase	Black and Brown Phases; Two Phase	Clear; Single Phase
FRT	0.22	0.58	0.76	1.00
Components				
C ₅ - C ₈	0.32	0.34	0.31	0.11
C ₉ - C ₁₂	0.27	0.24	0.29	0.44
C ₁₃ - C ₁₆	0.17	0.18	0.18	0.25
C ₁₇ - C ₂₀	0.11	0.12	0.11	0.11
C ₂₁ - C ₂₄	0.06	0.06	0.05	0.05
C ₂₅ - C ₂₈	0.04	0.04	0.04	0.02
C ₂₉ - C ₃₂	<u>0.02</u>	<u>0.02</u>	<u>0.02</u>	<u>0.02</u>
	1.00	1.00	1.00	1.00

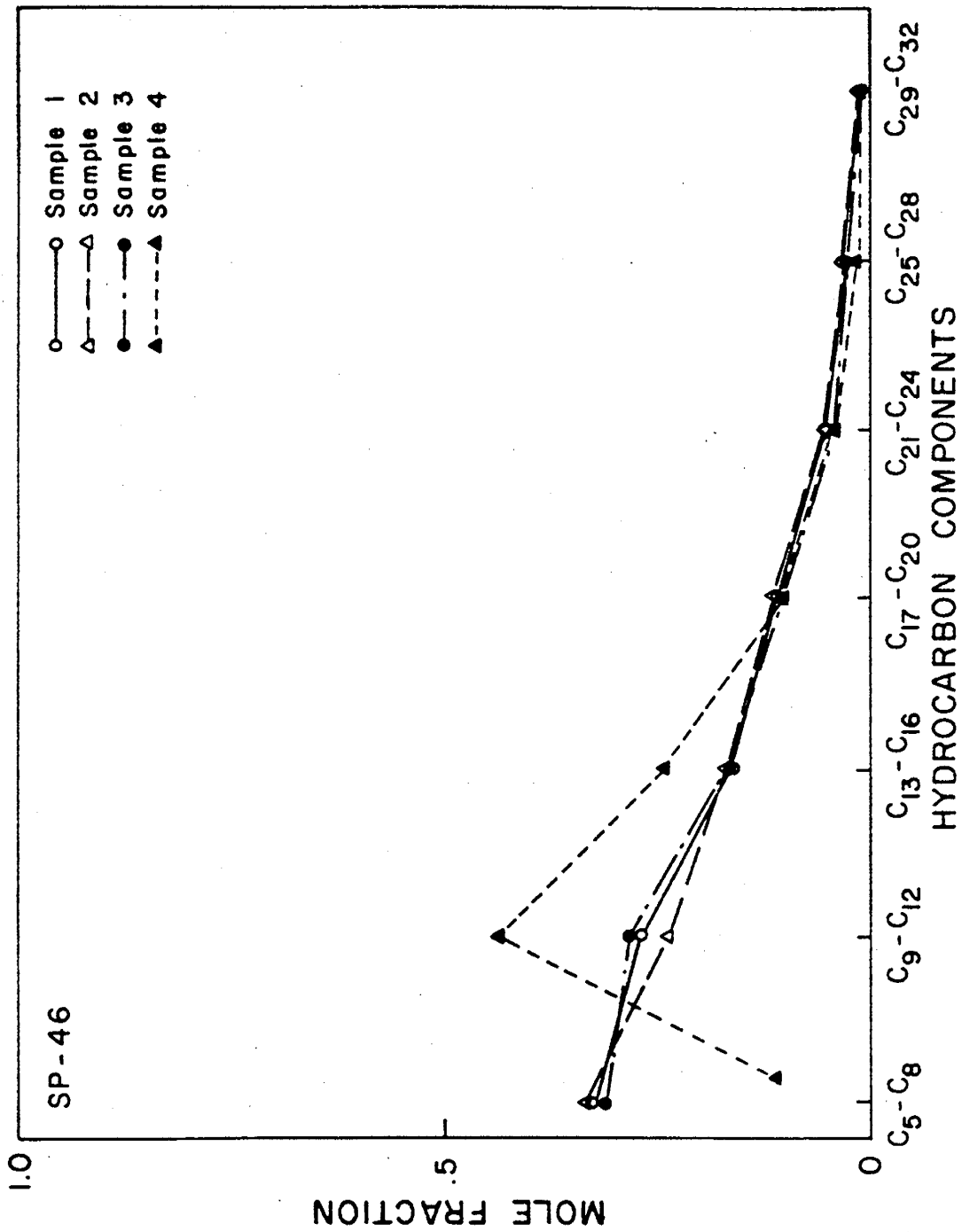


Figure 10. Composition of Brookhaven Crude Oil Samples from SP-46
(P = 2,900 psia, T = 140°F)

Table 11

Composition of Brookhaven Crude Oil Samples from SP-41
(mole fractions)

SP-41

P = 3200 psia

% Recovery: 86.1%

T = 140°F

Sample No.	1	2	3	4
Observations	Black; Single Phase	Black and Brown Phases; Two Phase	Yellow; Single Phase	Clear; Single Phase
FRT	0.24	0.75	0.85	0.98
Components				
C ₅ - C ₈	0.35	0.29	0.26	0.15
C ₉ - C ₁₂	0.25	0.31	0.35	0.45
C ₁₃ - C ₁₆	0.17	0.19	0.19	0.24
C ₁₇ - C ₂₀	0.11	0.10	0.10	0.10
C ₂₁ - C ₂₄	0.06	0.06	0.05	0.04
C ₂₅ - C ₂₈	0.04	0.03	0.03	0.01
C ₂₉ - C ₃₂	<u>0.02</u>	<u>0.02</u>	<u>0.02</u>	<u>0.01</u>
	1.00	1.00	1.00	1.00

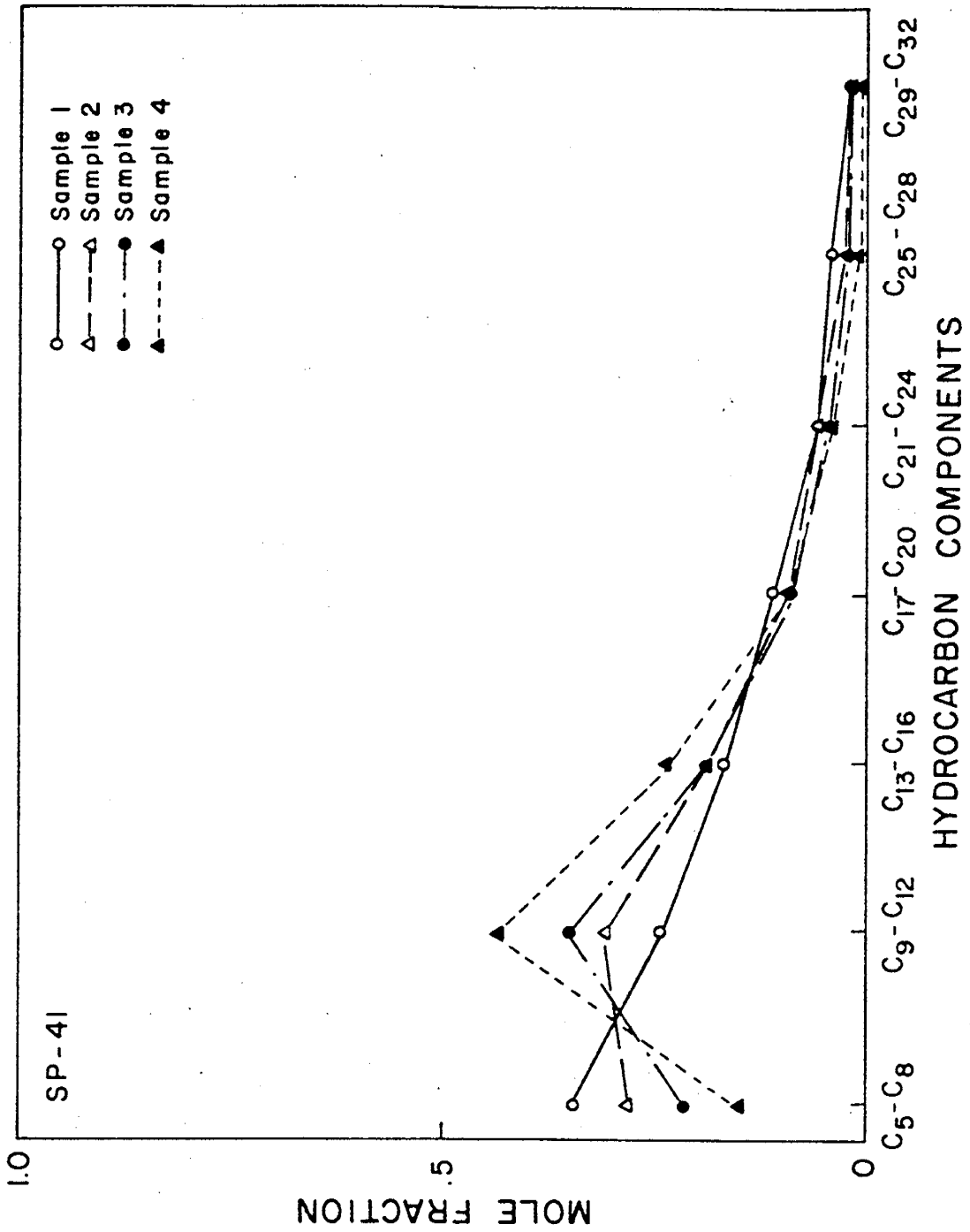


Figure 11. Composition of Brookhaven Crude Oil Samples from SP-41
(P = 3,200 psia, T = 140°F)

Table 12

Composition of Brookhaven Crude Oil Samples from SP-45
(mole fractions)

SP-45

P = 3800 psia

% Recovery: 92.8%

T = 140°F

Sample No.	1	2	3	4
Observations	Black; Single Phase	Black; Single Phase	Black and Brown Phases; Two Phase	Black; Single Phase
FRT	0.24	0.56	0.72	0.83
Components				
C ₅ - C ₈	0.27	0.20	0.22	0.17
C ₉ - C ₁₂	0.23	0.32	0.26	0.36
C ₁₃ - C ₁₆	0.22	0.21	0.24	0.22
C ₁₇ - C ₂₀	0.13	0.13	0.14	0.13
C ₂₁ - C ₂₄	0.07	0.07	0.07	0.06
C ₂₅ - C ₂₈	0.05	0.04	0.04	0.04
C ₂₉ - C ₃₂	<u>0.03</u>	<u>0.03</u>	<u>0.03</u>	<u>0.02</u>
	1.00	1.00	1.00	1.00

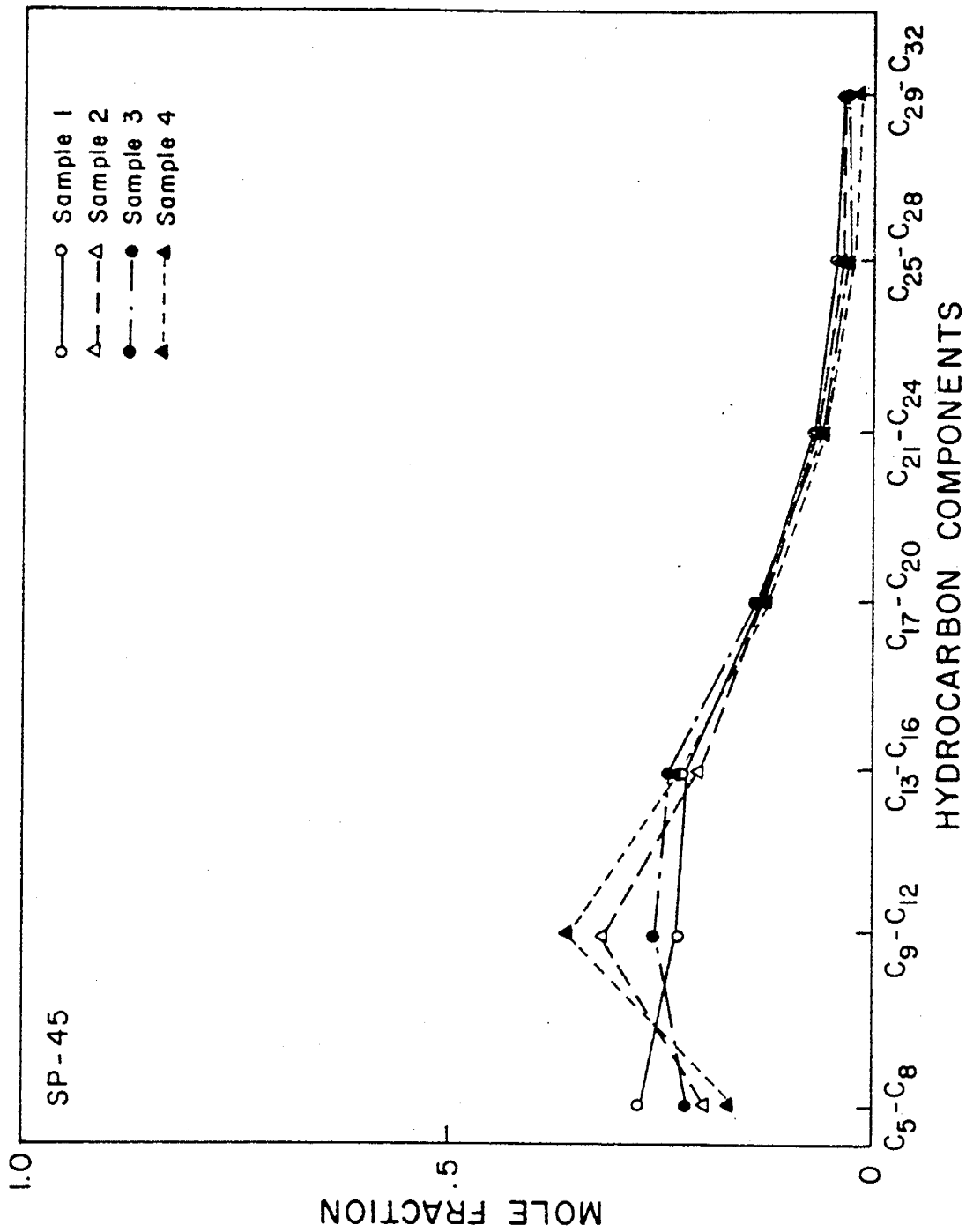


Figure 12. Composition of Brookhaven Crude Oil Samples from SP-45
(P = 3,800 psia, T = 140°F)

Table 13

Composition of Brookhaven Crude Oil Samples from SP-33
(mole fractions)

SP-33

P = 3200 psia

% Recovery: 92.8%

T = 109°F

Sample No.	1	2	3	4
Observations	Black; Single Phase	Black; Single Phase	Black and Clear Phases; Two Phase	Clear; Single Phase
FRT	0.19	0.54	0.82	0.94
Components				
C ₅ - C ₈	0.41	0.30	0.23	0.09
C ₉ - C ₁₂	0.18	0.28	0.35	0.40
C ₁₃ - C ₁₆	0.17	0.18	0.19	0.28
C ₁₇ - C ₂₀	0.12	0.12	0.12	0.13
C ₂₁ - C ₂₄	0.06	0.06	0.06	0.06
C ₂₅ - C ₂₈	0.04	0.04	0.03	0.03
C ₂₉ - C ₃₂	<u>0.02</u>	<u>0.02</u>	<u>0.02</u>	<u>0.01</u>
	1.00	1.00	1.00	1.00

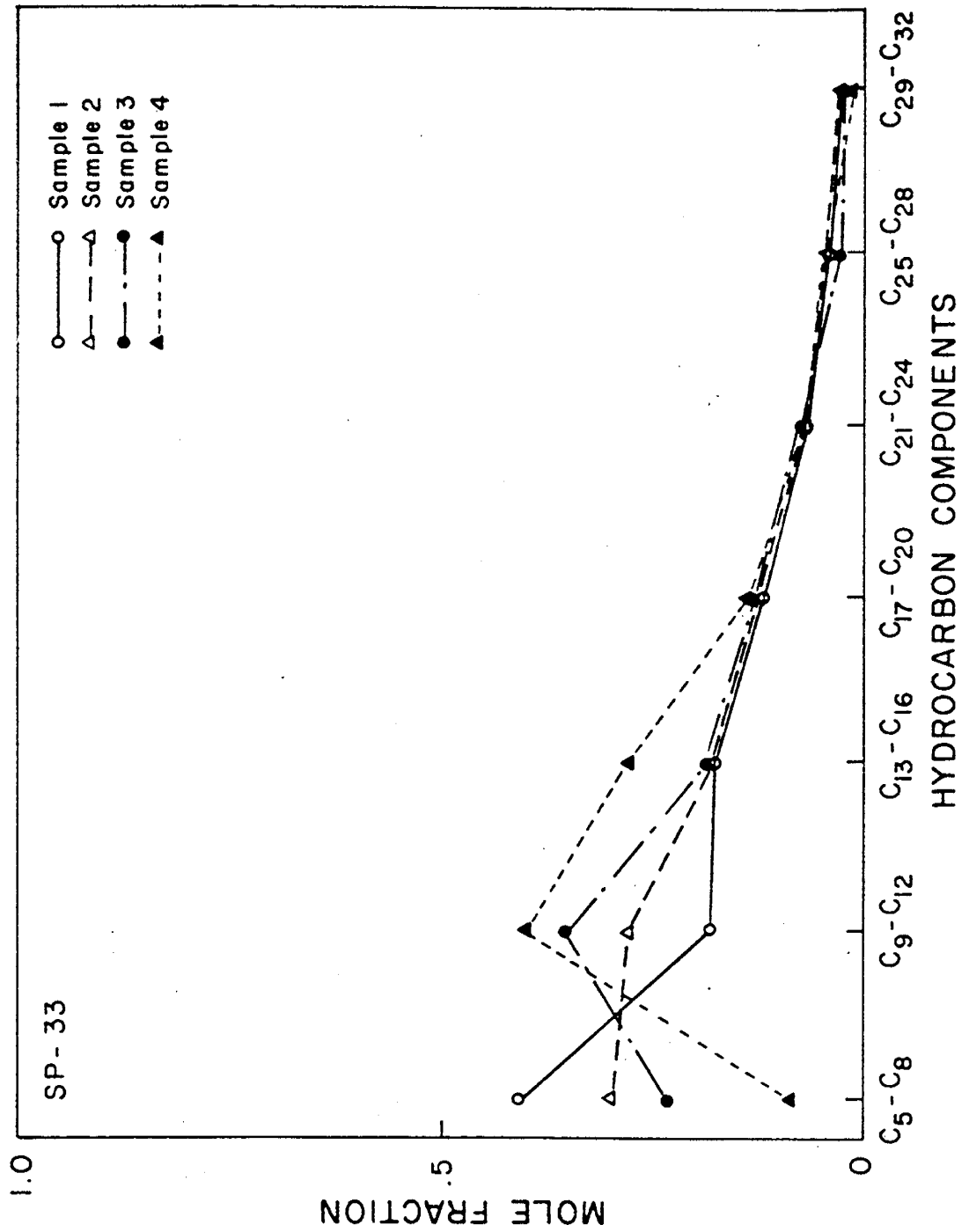


Figure 13. Composition of Brookhaven Crude Oil Samples from SP-33
(P = 3,300 psia, T = 109°F)

from one run to the next; however, apparent in all the later samples from these runs are the losses which have occurred in the heavier components, $C_{13} - C_{32}$. It appears then that compositional variations observed during these floods are uniform, regardless of the displacement pressure. It should be noted, however, that no samples were collected during the latter stages of these displacements (SP-49, SP-48, and SP-51) so that insufficient data concerning the composition of transition zone fluids was obtained.

Analyses of samples procured during SP-47 ($T = 175^{\circ}\text{F}$, $P = 3600$ psia) indicate a significant decrease in the $C_5 - C_8$ fraction of later samples. An appreciable increase is observed in the $C_9 - C_{12}$ fraction, and unlike the previous displacements, a slight increase is noted in the $C_{13} - C_{16}$ range. The improved oil recovery obtained at this pressure, 91.1%, appears to be related to the more efficient recovery of heavier hydrocarbons ($C_{13} - C_{16}$) in the transition zone. However, inadequate data concerning the composition of transition zone samples from most of the displacements at 175°F precludes a definitive conclusion pertaining to the compositional changes observed during the various CO_2 floods.

Sandpack displacements SP-43 ($P = 1800$ psia) and SP-39 ($P = 2200$ psia) were performed at pressures below the CO_2 MMP of Brookhaven crude oil at 140°F . The analyses of samples obtained from the transition zones of these floods indicate a significant decrease in the $C_5 - C_8$ fraction, with a concomitant increase in the $C_9 - C_{12}$ range. Little variation is noted in the $C_{13} - C_{16}$ fraction; however, significant decreases are observed in the heavier components, $C_{17} - C_{32}$. The ultimate recoveries from these displacements ranged from 72.8 - 79.6%.

According to Figure 1, SP-46 ($P = 2900$) was performed at the CO_2 MMP for this oil at 140°F . A significant decrease is noted in the $C_5 - C_8$ fraction with a corresponding increase being noted in the $C_9 - C_{12}$ fraction. In addition, an appreciable increase in the $C_{13} - C_{16}$ fraction is observed in the transition zone fluids of this displacement. Little variation is noted in the $C_{17} - C_{20}$ range, with decreases in the heavier fractions again being observed. The ultimate recovery from this displacement was 86.1%. Nearly identical compositional trends are observed for SP-41, which was performed at 3200 psia, a pressure just beyond the CO_2 MMP for Brookhaven crude oil. The ultimate recovery was, likewise, 86.1%.

SP-45, performed at 3800 psia and 140°F , unexpectedly yielded a greatly improved recovery approaching 93%. Analyses of samples obtained from this displacement indicate less dramatic compositional variation occurring in the transition zone fluids. The typically observed decrease in the $C_5 - C_8$ fraction and the increase in $C_9 - C_{12}$ fraction are less pronounced. Little change is exhibited in the $C_{13} - C_{20}$ range, with only slight decreases being observed in the $C_{21} - C_{32}$ range. It should be noted, however, that the last sample was obtained at 0.83 FRT and may not indicate what compositional variations occurred earlier in the developing transition zone.

Only one adequate series of samples were obtained from the sandpack displacements at 109°F . This run, SP-33, was performed at 3200 psia, and the ultimate recovery was 92.8%. Typically, samples obtained from the transition zone of the displacement indicate significant decreases in the $C_5 - C_8$ fraction with corresponding increases in the $C_9 - C_{12}$ range. Most important,

however, is the efficient recovery of hydrocarbon components through the C₂₁ - C₂₄ fraction.

The compositional analyses of all transition zone samples, obtained from the sand pack displacements at 140°F, indicate significant losses in the C₅ - C₈ fraction. It is believed, however, that the decreases observed are the result of the high volatility of these components rather than the result of a particular displacement mechanism. Samples obtained from displacements performed below the CO₂ MMP at 140°F indicate that the major components extracted into the CO₂-rich phase of transition zone fluids lie in the C₉ - C₁₆ range. Less efficient extraction of the heavier hydrocarbons at these pressures results in components, within the C₁₇ - C₃₂ range, being left behind the developing transition zone. Analyses of samples obtained from displacements at pressures near the CO₂ MMP at 140°F indicate that the depth of CO₂ extraction has increased to include hydrocarbons in the C₁₇ - C₂₀ range, as well as the C₉ - C₁₆ fraction. Concurrent with the deeper extraction observed in these displacements are the improved recoveries noted in SP-46 and SP-41. The most apparent feature in the compositional profiles of samples obtained from SP-45 and SP-33 appears to be the increased recovery of heavier hydrocarbon components in the transition zone fluids.

According to Figure 1, as the displacement temperature increases, higher pressures are required to effect equivalent recoveries of oil. This confirms that the efficiency of the CO₂ displacement mechanism is a function of the CO₂ density as has been stated by Holm and Josendel (1982). As the pressure increases, for a particular temperature, the compositional profiles of the transition zone fluids reflect the improved recovery of heavier hydrocarbon components. It appears then that as the density of CO₂ increases, its ability to extract heavier hydrocarbons also increases resulting in improved ultimate recoveries. As improved hydrocarbon extraction proceeds, additional evidence suggests that aromatics concentrate in the stripped oil to promote deposition of a solid phase. Visual observations during the sandpack displacements confirmed that a solid phase formed with the generation of miscibility. Since solid phase formation was also observed during immiscible runs it does not reflect the attainment of miscibility. The solid phase was somewhat mobile, and appears to be related to the atypical "S" shape of the ultimate recovery versus pressure curves recorded at high temperatures (Figure 1). Various amounts of solid phase were produced during all the Brookhaven sandpack displacements. Compositional analyses of effluent samples collected during sandpack displacements suggested that the solid phase represents a small mass fraction of the total oil production. Table 14 presents a typical compositional profile for effluent samples collected during SP-47. The data show a continuous hydrocarbon fractionation as the displacement progressed, characterized by lighter component enrichment and heavier component depletion. The molecular weight and aromatic carbon content of the effluent decreased throughout the run, suggesting that during the MCM process, the aromatics concentrate in the stripped oil. This perhaps catalyzes solid phase formation. The amount of solid phase present in sample number 2 was apparently insufficient to influence the recorded compositional trends.

CONCLUSIONS

1. The results of sandpack displacements of Brookhaven reservoir oil, detailed in this contract's Annual and Final reports, support a

Table 14

ANALYSES OF EFFLUENT FROM CO₂-BROOKHAVEN OIL SANDPACK DISPLACEMENT^a

Sample No.	1	2	3	4
<u>Sight Glass Observations</u>	Black; Single liquid Phase.	Brown liquid with black solid-like residue.	Brown; Single liquid Phase.	Clear; Single liquid Phase.
<u>FRT</u> ^b	0.29	0.77	0.88	0.98
<u>Compositions</u>				
C ₉ - C ₁₂	0.313	0.376	0.448	0.478
C ₁₃ - C ₁₆	0.301	0.286	0.256	0.273
C ₁₇ - C ₂₀	0.182	0.164	0.152	0.140
C ₂₁ - C ₂₄	0.095	0.083	0.078	0.062
C ₂₅ - C ₂₈	0.064	0.054	0.044	0.032
C ₂₉ - C ₃₂	<u>0.045</u>	<u>0.037</u>	<u>0.022</u>	<u>0.015</u>
	1.000	1.000	1.000	1.000
<u>Molecular Weight</u> ^c	241	238	214	202
<u>Aromatic Carbon</u> ^d	13%	9%	9%	7%

a Run conditions 353°K, and 24820 kPa gage pressure at sandpack exit.

b Fractional run time for run terminated at GOR = 30,000 SCF/STB.
CO₂ breakthrough occurred at 0.74 FRT.

c Determined by gas chromatography following proposed ASTM standard
(g/g-mol).

d Determined by ¹³C NMR.

general picture of the dominant factors which influence the MMP in the CO₂ gas miscible displacement process. Temperature usually has the primary effect, with oil compositional effects of lesser magnitude. The relative importance of the type of oil compositional effect depends upon flood conditions. Three types of oil compositional effects were demonstrated by the displacement experiments completed under this contract, namely, hydrocarbon molecular weight distribution, oil aromaticity, and solution gas.

2. Increasing the temperature increases the required MMP. The MMP temperature dependence was more pronounced in dead oil versus live oil displacements (Monger and McMullan, 1983). This MMP difference, attributed to the effects of solution gas, diminished with increasing temperature.
3. The influence of hydrocarbon molecular weight distribution is reflected by compositional analyses of effluent samples from displacements performed at a given temperature. At lower pressures the major components extracted into the CO₂-rich phase are in the C₉-C₁₂ range. As the run pressure is increased to approach the MMP, the ability of CO₂ to extract heavier hydrocarbons improves, thereby achieving greater oil recoveries. An increase in the proportion of intermediate molecular weight hydrocarbons allows sufficient extraction to occur at a lower pressure, because CO₂ preferentially solubilizes these hydrocarbons. This explains the well-known observation that for a given temperature the MMP increases with increasing crude oil molecular weight.
4. As improved hydrocarbon extraction into a CO₂-rich phase proceeds, aromatics concentrate in the stripped oil to promote deposition of a solid phase. How this solid phase will affect oil recovery on a reservoir scale is unclear, but potential benefits from mobility control and/or wettability change deserve further investigation.
5. The effects of solution gas are mixed. The presence of methane has little effect on the MMP. Sandpack displacements of live Brookhaven oil show that methane is expelled from the crude by CO₂ and moves ahead of the flood front because of its high mobility (Whitehead et al., 1981). Dissolved methane is thus expected to have little impact on the CO₂ gas miscible displacement process for frontal velocities which are not gravity stable. The presence of other light hydrocarbons, however, tends to lower the MMP (Monger and McMullan, 1983).

PART II - COREFLOODS USING CARBON DIOXIDE WITH SYNTHETIC OR NATURAL RESERVOIR OIL SYSTEMS

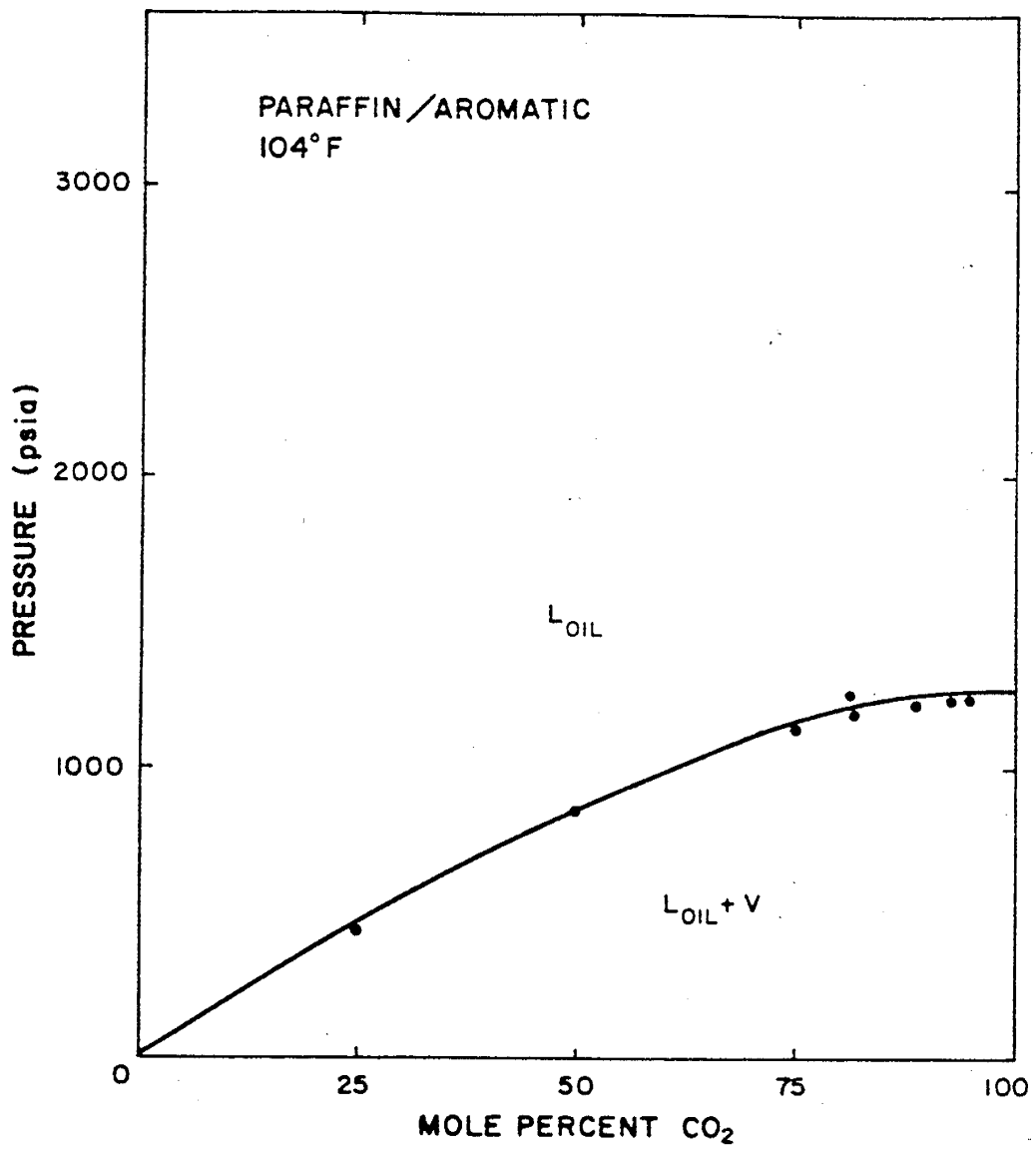
INTRODUCTION

In addition to molecular weight and hydrocarbon distribution, the type of hydrocarbons (paraffin/aromatic) present in the crude oil influences the CO₂ displacement process. Higher oil recovery and lower MMP from a sandpack displacement of oil having increased aromatic content has been reported (Holm and Josendal, 1982). Monger and Khakoo (1981) hypothesized that hydrocarbon extraction into a CO₂-rich phase improves with increasing crude oil aromaticity. The following analyses were performed in order to assess the effect of varying oil composition, in particular the presence of aromatic components, on the recovery efficiency and phase behavior observed during CO₂ displacement of oil. This portion of the investigation consists of a two part study involving:

- (1) tertiary CO₂ corefloods with several synthetic oils and
- (2) compositional analyses of synthetic oil samples obtained during the corefloods.

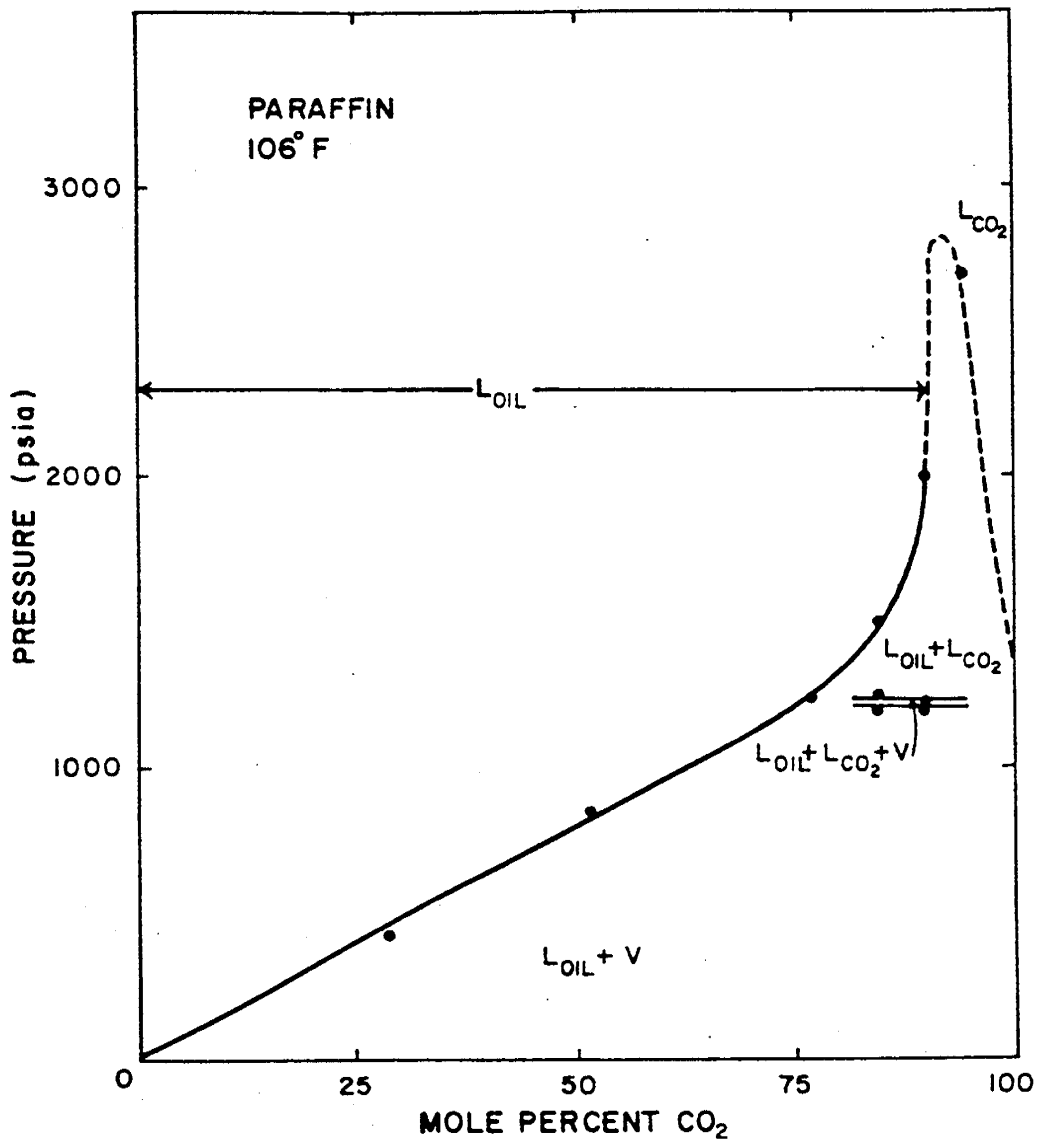
A total of nine tertiary corefloods (six of which were successful) were performed using synthetic oils designed to model the phase behavior exhibited by naturally occurring crude oils. The synthetic oils were selected to facilitate the examination of compositional effects on CO₂/crude oil interactions (Monger and McMullan, 1983). The floods were performed at approximately 100°F and 1300 psia. These conditions were chosen so as to enable the study of FCM and MCM displacements, based on the pressure-composition (P-X) diagrams reported for these synthetic oils (Figures 14 - 16). According to the P-X diagrams, these flood conditions also enable the observation of liquid-liquid equilibria at high concentrations of CO₂ (Figures 15 and 16). Results of these corefloods include secondary water flood recoveries, residual oil saturations, and tertiary CO₂ flood recoveries. Compositional analyses on synthetic oil samples obtained at various points during the floods and accompanying phase observations are also reported.

There have been numerous experimental and mathematical studies of viscous fingering in first-contact miscible solvent/oil systems (Stalkup, 1983). Briefly, displacing fluid viscosity is less than displaced fluid viscosity and finger initiation is attributed to the presence of permeability heterogeneities in an essentially homogeneous porous media. Once fingers above a critical wavelength are initiated, finger growth depends upon the importance of dispersion in the displacement. In the case of dipping reservoirs, gravity segregation can dampen finger development (Blackwell et al., 1959; Lacy et al., 1958; Slobod and Howlett, 1964). To prevent viscous fingering in the strictest sense, the displacement rate must be below the "stable rate" described by Dumore (1964). In practice, the "critical rate" as described by Hill (1949) may be an adequate criterion.



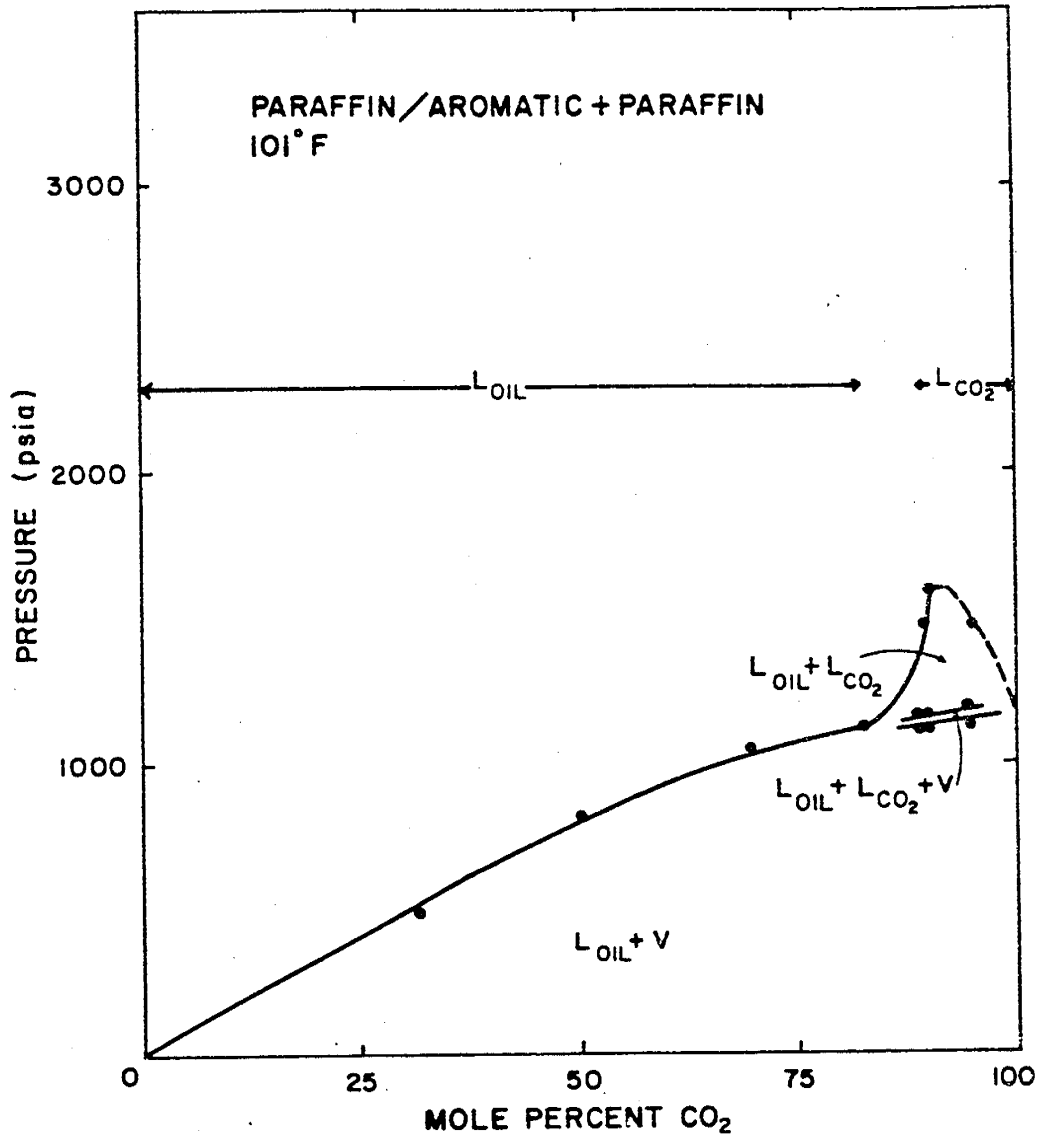
(after Monger et al.²²)

Figure 14. Pressure-Composition (P-X) Diagram of Oil P/A



(after Monger et al.²²)

Figure 15. Pressure-Composition (P-X) Diagram of Oil P



(after Monger et al.²²)

Figure 16. Pressure-Composition (P-X) Diagram of Oil P/A-P

Although the behavior of viscous fingers has been of interest to the oil industry for many years, it is not clear whether the mechanics of viscous fingering derived using first-contact miscible systems apply to the multiple-contact miscible displacement of oil by CO₂. Gardner and Ypma (1984) have shown, for example, that there is a synergistic interaction between multiple-contact CO₂-crude oil phase behavior and viscous fingering that further limits ultimate oil recovery. Gardner and Ypma's work neglected gravity effects, but it is reasonable to expect that CO₂-crude oil phase behavior will also influence the behavior of viscous fingers in the presence of gravity segregation. Component partitioning between injection fluid and oil in place certainly affects calculations of displacement rates. Assuming that the equations of Dumore and Hill are applicable to CO₂ flooding, the choice of appropriate solvent/oil permeabilities, viscosities and densities are extremely complex due to the transition zone established by the multiple-contact mechanism. The focus of this research plan is to provide laboratory coreflood and supportive PVT data which will facilitate the design of a gravity stable, multiple-contact miscible CO₂ flood and lead to improved prediction of critical displacement rates. As far as implementation of a gravity stable, multiple-contact miscible CO₂ flood is concerned, recent field tests are providing encouraging results from a technical standpoint (Palmer et al., 1984; Cardenas et al., 1984; Perry, 1982). From an economical standpoint, however, the benefits of improved oil recovery are threatened by the long lead times imposed by gravity stable injection rates. An additional aim of this research plan is to quantitate the incremental oil recovered with injection rate reduction for a reservoir that is a candidate for implementation of a gravity stable, multiple-contact miscible CO₂ flood.

EXPERIMENTAL SECTION

Horizontal Corefloods Using Carbon Dioxide and Synthetic Oil Systems

Core Apparatus

The corefloods were performed in two 6 ft. long, 2 inches in diameter Berea sandstone cores. Figure 17 is a schematic of the horizontal coreflood apparatus. The pore volumes and permeabilities of the cores are provided in Table 15. The cores were horizontally aligned and during the floods were mechanically rotated in an effort to minimize gravity segregation. The cores were maintained at approximately 100°F during floods by continuously circulating water of constant temperature through copper coils surrounding the cores. The temperature of the water was held constant using a Y.S.I. Model 72 proportional temperature controller. Inlet and outlet pressures were monitored using Bourdon tube pressure gauges, and a Tescom back-pressure regulator (BPR), tested to 6000 psi, was used to maintain the outlet pressure at 1300 psia. A sight-glass mounted on a panel at the outlet end of the cores enabled visual observations to be performed at flood conditions, throughout each of the runs. The measurement of produced gas was accomplished using a calibrated wet test meter from Precision Scientific.

Synthetic Oils

The synthetic oils used in this study are the same synthetic oils discussed in Volume I of this report. They consisted of a 100% paraffinic oil (P), a 50% paraffinic/50% aromatic oil (P/A), and a 50-50 blend of the 100%

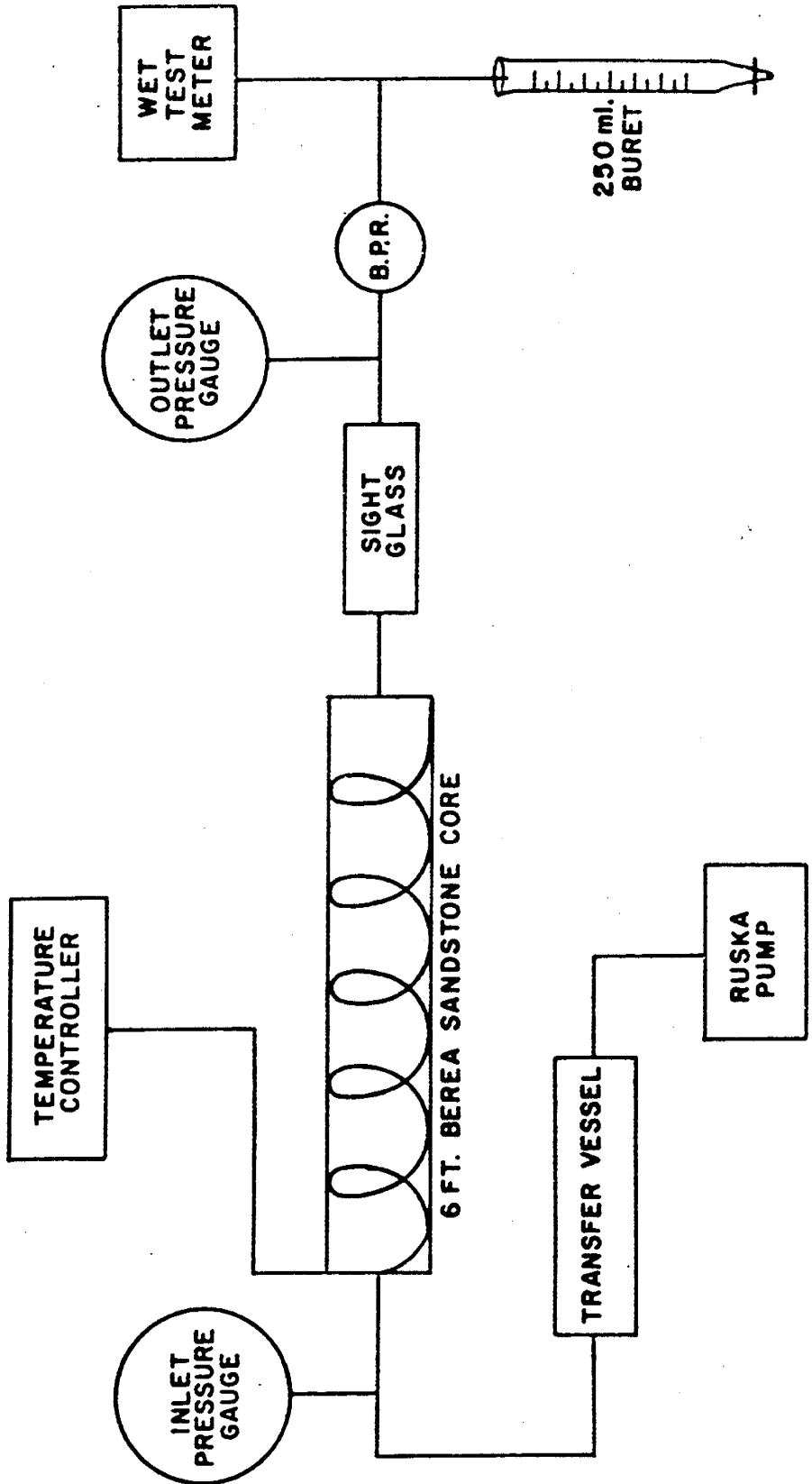


Figure 17. Schematic of Core Apparatus

Table 15

Pore Volumes and Permeability
of Berea Sandstone Cores

Core	Pore Volume	Permeability
2	815 cc	299 md
3	875 cc	248 md

paraffinic oil and the 50% paraffinic/50% aromatic oil (P/A-P). The compositions, molecular structures, and physical and chemical properties of these oils are presented in Tables 16 - 18. The oils were prepared gravimetrically by weighing appropriate amounts of each component into airtight glass containers. They were then refrigerated until needed. Prior to each flood, the oils were allowed to stand at room temperature until all components were completely dissolved. At this point the oils were shaken, filtered, and loaded into the transfer vessel.

Brine Solutions

The brine solutions used in this experiment consisted of a 50,000 parts per million (ppm) solution of sodium chloride (NaCl) and a 20,000 ppm NaCl solution. These solutions were prepared by dissolving appropriate amounts of NaCl in distilled water.

After the second CO₂ displacement, 10 weight per cent CuSO₄ was added to the 50,000 ppm NaCl solution used to flush the core. The purpose of this addition was to color the aqueous phase in an attempt to facilitate visual observations. Undissolved material caused excessive pressure build-up during the following displacement, and use of CuSO₄ was, therefore, discontinued.

Pumps and Transfer Vessels

Brine solutions and IPA were pumped directly into the core using a Whitey feed pump. A single-barrel Ruska proportioning pump was used to volumetrically displace synthetic oils and CO₂ from high-pressure transfer vessels into the cores at a constant rate. The transfer vessels consisted of 2 to 2½ ft. long and 3½ to 4½ inch outside diameter, thick-walled, stainless steel cylinders equipped with floating pistons. Buna-N O-rings were used to provide pressure seals and to prevent contamination of the synthetic oils and/or CO₂ by the hydraulic fluid.

Experimental Procedure

The cores were initially prepared for the subsequent floods using a preliminary cleaning procedure which consisted of:

- (1) flushing with one pore volume (PV) 20,000 ppm brine;
- (2) flushing with one PV isopropyl alcohol (IPA);
- (3) a second flushing with one PV 20,000 ppm brine;
- (4) flushing with 4-5 PV 50,000 ppm brine to a water saturation (S_w) close to 1.0. This was accomplished by flushing the core with 50,000 ppm NaCl until the producing GOR was less than 1 SCF/STB; and, there was no visible production of oil and no smell of IPA in the effluent stream.

This procedure was repeated following each core flood, while a back pressure of approximately 1,000 psi was maintained to prevent the flashing of gaseous CO₂ within the core.

Table 16

Synthetic Oil Compositions

	Paraffinic (P)	Paraffinic/Aromatic (P/A)	Synthetic Blend (P/A-P)
C ₅	20 mol % Pentane	20 mol % Pentane	20 mol % Pentane
"C ₁₀ "	50 mol % Decane	30 mol % Decane 20 mol % n-Butyl- benzene	40 mol % Decane 10 mol % Butyl- benzene
"C ₂₀ "	20 mol % Eicosane	20 mol % 2-Methyl- naphthalene	10 mol % Eicosane 10 mol % 2-Methyl- naphthalene
"C ₃₀ "	10 mol % Squalane	10 mol % Biphenyl	5 mol % Squalane 5 mol % Biphenyl

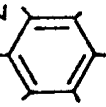
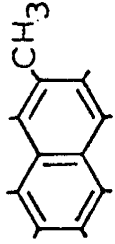
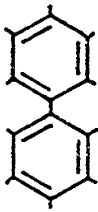
Table 17

Synthetic Oil Molecular Structures

"C₃₀"

"C₂₀"

"C₁₀"

<p>CH₃(CH₂)₈CH₃</p>	<p>CH₃(CH₂)₁₈CH₃</p>	<p>hexamethyl- CH₃(CH₂)₂₂CH₃</p>
<p>CH₂(CH₂)₂CH₃ </p>	<p></p>	<p></p>

PARAFFINIC

AROMATIC

Table 18

Properties of Synthetic Oils

	<u>P/A</u>	<u>P</u>	<u>P/A-P</u>
<u>Molecular Weight</u>			
(g/mol)	128	184	156
<u>Density</u>			
(g/cc)			
(70°F, 1 atm)	0.823	0.756	0.780
(100°F, 1500 psia)	0.819	0.752	0.776
<u>Viscosity</u>			
(cp)			
(70°F, 1 atm)	1.133	2.274	1.537
<u>Carbon Type</u>			
(paraffin)	53%	100%	80%
(aromatic)	47%		20%

Prior to the initiation of all floods, except for Runs 2 and 4, the water-saturated core was brought to run temperature (approximately 100°F) and allowed to stabilize overnight. A constant back pressure of 1300 psia was held on the core effluent; while, approximately two-thirds pore volume of the appropriate synthetic oil was loaded into the core at a rate of 400 cc/hr. (Only a fractional pore volume of the synthetic oil was loaded into the core, as opposed to establishing an irreducible water-saturation, for economic reasons.) In each case, 400-500 cc of oil remained in the core. This amount was calculated volumetrically by subtracting the volume of oil produced at atmospheric pressure from the total volume of oil metered into the core, which was measured directly from the Ruska pump at run pressure. No corrections were made for compressibility changes or thermal expansion as the synthetic oil was dead, and these effects are considered negligible. The core was then flushed to near residual oil saturation (S_{OR}) by flooding with 50,000 ppm brine at a rate of 300-400 cc/hr. until the apparent production of oil ceased. The S_{OR} was calculated by subtracting the volume of oil produced at atmospheric pressure from the amount of oil which remained in the core after the loading procedure. It should be noted here that the S_{OR} determined in this manner is not a unique value, as this would necessitate continued flooding with brine over an extended period of time. For Runs 2 and 4, the core was loaded and flushed to S_{OR} at room temperature, and was then brought to run temperature and allowed to stabilize overnight.

The tertiary CO_2 flood was begun at this point. At room temperature and run pressure, CO_2 was pumped into the core at a fixed rate of 100 cc/hr. Typically, brine was produced during the early portion of the displacement, followed by a period in which oil and brine were produced simultaneously. Differential pressures encountered in Core 3 during this portion of the flood usually ranged from 100-120 psi, tapering gradually to approximately 80 psi as the oil/brine ratio increased. At CO_2 breakthrough (BT), the differential pressure had decreased to approximately 50 psi and continued to decline as production became predominantly oil. As the flood progressed, CO_2 production increased steadily, and the differential pressure dropped to 15-20²psi. While the same sequence of events were noted during the displacements in Core 2, the differential pressures encountered were slightly higher.

Under ambient conditions, produced oil and water were collected in a series of 5 to 7 100 ml. graduated cylinders, covered, and allowed to settle overnight to facilitate separation prior to measurement. Produced gas was measured directly at atmospheric conditions using the wet test meter. Throughout the displacements, other pertinent data was recorded, including: the cc's of CO_2 injected; cc's of CO_2 injected at the time of CO_2 BT; producing gas/oil ratios (GOR); pressure changes; and visual observations of the effluent phase behavior. Samples of the synthetic oil phase, which separated from the produced fluids pooled in the graduated cylinders, were collected in airtight glass vials and refrigerated pending their compositional analyses. The floods were terminated when the producing GOR exceeded 30,000 SCF/STB.

Compositional Analyses Performed for Corefloods Using Synthetic Oils

Samples and Standards

Samples obtained from the previously discussed tertiary core floods were refrigerated in airtight glass vials. Just prior to analyses, the samples

were allowed to stand at room temperature for approximately one hour in order to redissolve solidified components and to ensure a well-mixed sample for injection.

Small samples of each of the original synthetic oils (Table 16) were retained as standards for the subsequent compositional analyses.

Apparatus

The compositional analyses were performed using the Hewlett Packard 5880 gas chromatograph, as described in Part I, Experimental Section, Apparatus. The columns consisted of 4 ft. long, $\frac{1}{4}$ inch outside diameter Nickel-200 columns, packed with 5 per cent OV 101 on Chromosorb W. These columns were prepared for the analyses employing the conditioning procedure previously described. The 99.995 per cent pure Helium carrier gas was adjusted to flow rates of 40 cc/minute \pm 0.5 cc, and injections were made with a 10-microliter Hamilton gas-tight syringe.

Time/Temperature Program

Because the synthetic oils contained significant amounts of pentane and no components heavier than C_{30} , the time/temperature program employed varied slightly from the program used for analyzing the dead Brookhaven crude oil samples.

Oven Temperature Profile:

Initial Value	=	0°C
Initial Time	=	2.00 minutes
Program Rate	=	10°C/minute
Final Value	=	340°C
Final Time	=	15.00 minutes

The injection port temperatures and the detector temperatures were maintained at 300°C and 370°C, respectively. Throughout the testing period, the columns were baked overnight at 340°C, in an effort to minimize any residual sample contamination.

Sample Analyses

The synthetic oil samples were analyzed by first injecting a two microliter sample of the standard synthetic oil in order to calculate response factors (RF). The RF, which correct for differences in the sensitivity of the detector to different sample components, are defined as:

$$\text{Response Factor (RF)} = \frac{\text{calibrated amount}}{\text{calibrated area}}$$

In these analyses, "calibrated amount" consisted of the actual weight in grams of a particular component in the 2 microliter sample of the standard and "calibrated area" was simply the area counts associated with the corresponding chromatographic peak.

The calculated RF were used to convert the area counts of subsequent synthetic oil samples to grams. The weights of each component were then converted to moles and finally to mole fractions.

Vertical Corefloods Using Carbon Dioxide and Timbalier Bay Reservoir Oil

Core Apparatus

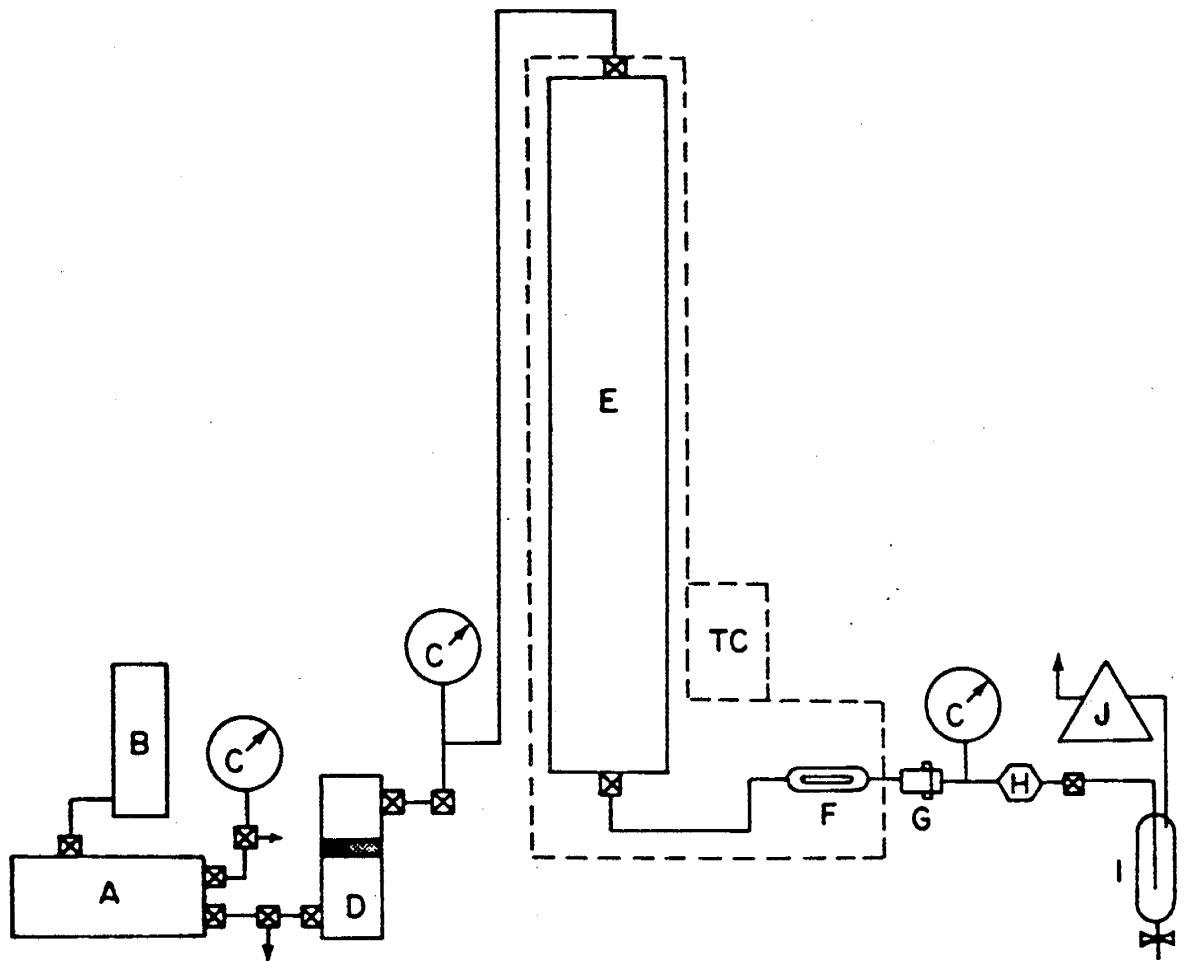
A photograph of the vertical coreflood apparatus has been reported previously (Monger and McMullan, 1983). Figure 18 is a schematic of the vertical coreflood apparatus. Timbalier Bay reservoir oil corefloods were performed using six feet long, 2-inch diameter Berea sandstone cores. Stainless steel end caps, tapped for tubing connections, were fastened to the ends of the core. The core was coated with Armstrong C-7 epoxy resin to maintain a linear flow path through the core. The core was installed in a 10 feet long cylindrical steel pressure vessel; the resulting annular space was partially filled with hydraulic oil and pressurized with a nitrogen cap. The ends of the pressure vessel were fitted with threaded plugs tapped for tubing connections and utilizing O-ring seals of a compound stable at high temperature and pressure. The pressure vessels were wrapped with copper tubing. A centrifugal pump was used to circulate a water/ethylene glycol mixture from a standard water heater through the copper tubing which was insulated against heat loss. A counter-flow heat exchanger was installed in the system to preclude temperature differentials across the core.

Timbalier Bay Reservoir Oil

The Timbalier Bay stock tank oil used in this study was provided by Gulf Oil Exploration and Production Company and was obtained from Timbalier Bay State Lease 192 "PP" No. 280. Bubblepoint pressure is about 4500 psia at the 206°F reservoir temperature. Phase behavior measurements indicated that the reservoir fluid behaves as a medium shrinkage oil having a solution gas-oil ratio of 818 SCF/STB and a formation volume factor of 1.425 RB/STB at its bubble point. Additional properties of Timbalier Bay stock tank oil are summarized in Table 19.

Experimental Procedure

Fluids were pumped through the core during corefloods by a Ruska dual-cylinder proportioning pump. Injection rate was held constant at 100 cm³ per hour. A steel transfer vessel containing a floating piston was used to segregate the working fluid of the pump (hydraulic oil) from the crude oil or carbon dioxide. Tubing of 1/8 inch diameter connected the various components of the system. The core upstream and downstream pressures were continuously monitored from a panel near the pressure vessel. The panel also utilized a back-pressure regulator rated at 6000 psi, a wet test meter for measuring effluent gas volume, a buret of 250 cm³ capacity for measuring effluent liquid volume, and a liquid sampling device. A high pressure, back-lighted sight glass was placed upstream of the back pressure regulator to provide a means of



- | | |
|---|------------------------------------|
| A - Positive Displacement Pump | E - Consolidated Core |
| B - Storage Reservoir | F - Sight Glass |
| C - Pressure Gage | G - Sampling Yoke |
| D - Floating Piston Transfer Vessel | H - Back Pressure Regulator |
| TC - Temperature Controller | I - Flash Separator |
| → To Vent, Vacuum, or Compressed Gas | J - Wet Test Meter |

Figure 18. Schematic of Vertical Coreflood Apparatus

Table 19

Properties of Timbalier Bay Stock Tank OilMolecular Weight

freezing point depression	222 g/g-mol
gas chromatography	224 g/g-mol

Density

API gravity	32.4
specific gravity	0.8633

¹³C NMR Carbon Content

saturated carbon	88%
unsaturated carbon	12%

observing the phase behavior of the effluent. The corefloods were terminated when the measured gas/liquid ratio reached or exceeded 30,000 SCF/STB.

Our continuing series of corefloods has been interrupted due to suspected instability of the resin/activator mixture at 200°F, and the failure of O-ring seals which allowed internal core pressures to exceed the annular pressure. Remedies to date for these problems have been to use O-rings of a more durable compound, and to use newly-purchased resin and activator. In-house experiments indicate that the new resin and activator, Armstrong C-7, when mixed in proper proportions, yields a stable mixture near 212°F. Unfortunately, the core assembly with the resin in place can only be tested after the core has been installed inside its core holder.

The results of Run 2 which used Core 1 (see Results and Discussion), indicated that traces of oil from a previous run had not been removed from the core prior to the flood. This initiated a more effective core cleaning procedure which was then followed after each subsequent run. The cleaning procedure includes displacement through the core of the following fluids:

- 1 pore volume 2% NaCl solution
- 1 pore volume isopropyl alcohol
- 1 pore volume toluene
- 1 pore volume isopropyl alcohol
- 1 pore volume 2% NaCl solution
- 1 pore volume 5% NaCl solution

The volume of each fluid in the cleaning procedure is not critical; the effluent was observed for traces of oil after each step, and slight adjustments in the procedure were made as needed.

Before Run 4 which used Core 1 (see Results and Discussion), core permeability was determined by making precise measurements of rates of effluent production under specific pressure drops. Since the core assembly is mounted vertically and displacement through the core proceeds in a downward direction, Darcy's equation including the term for gravity effects was used to calculate permeability, also using the measured parameters. The equation used was

$$v = \frac{q}{A} = \frac{-k}{\mu} \left(\frac{\Delta P}{\Delta S} - 9.67 \times 10^{-4} \rho \cos \theta \right),$$

where

v = fluid velocity in cm/sec

q = flow rate in cm³/sec

A = cross-sectional area in cm²

k = permeability in darcies

μ = fluid viscosity

ΔP = pressure drop in atmospheres

ΔS = core length in cm

ρ = fluid density in gm/cm³

θ = angle of deviation from vertical of flow path

The initial permeability measurement was about 40 millidarcies (md). After Run 4 the permeability had been reduced to about 20 md, indicating some plugging of the core due possibly to formation of precipitates during the run. A backflush procedure using the same sequence of fluids as the normal cleaning procedure was then performed, which raised the measured permeability back to about 40 md. Since typical values of the permeability of Berea sandstone are an order of magnitude greater than 40 md, it was concluded that the core had been damaged by previous displacements, and another core was prepared for use.

Core 2 was prepared as follows. End caps were first installed on the core using the the resin/hardener mixture. The core was mounted in the core holder and the annular space was filled with hydraulic oil. An N₂ cap was injected into the annular space, and dry N₂ was displaced through the core overnight. The core was then evacuated with a vacuum pump. NaCl solution (5%) was allowed into the core; the volume of NaCl solution required to fill the core was then the pore volume of the core. The resulting porosity was calculated as 19%. Permeability was measured as for the previous core at about 80 md. The core was cleaned following the standard procedure. A CO₂ flood was performed under secondary recovery conditions (see Results and Discussion). While the core was pressurized prior to a second coreflood, an O-ring seal on the pressure vessel failed, allowing the annular pressure to fall below the internal core pressure. The result was a burst core, which necessitated preparation of Core 3.

Core 3 was prepared using new more durable O-rings and the same procedure as for the previous core assembly. Porosity was measured at about 20% and permeability at about 145 md. While performing an in-place pressure check of the system, hydraulic oil was observed in the effluent stream, the source of which was apparently the annular space around the core. Inspection revealed that the resin used to seal the end caps on the core had "flowed" at high temperature. Evidently the resin and/or hardener had expired significantly before their indicated shelf lives. Core 3 is currently being repaired and prepared for continuing corefloods. A new resin/hardener has been tested and appears to be stable at temperatures above 200°F. The core will be shortened about 3 inches and the end caps reattached. The same cleaning and measurement procedures will be followed prior to resuming the corefloods.

RESULTS AND DISCUSSION

Corefloods Using Synthetic Oils

Numerous sight-glass blow-outs occurred during Runs 1 and 2, resulting in severe pressure surges and production losses. Excessive pressure differentials, probably due to CuSO₄ plugging, were exhibited throughout Run 3 and necessitated continuous lowering of the CO₂ injection rate. These three

displacements, Runs 1, 2, and 3, were considered unsuccessful. The results obtained from these floods are presented in Table 20; however, no attempt was made to discuss or interpret this data. Results of the successful corefloods are presented in Table 21, and discussed in the following section.

Variations in the water flood recoveries (WFR), residual oil saturations (S_{OR}), and CO_2 BT for floods performed with the same oils in cores 2 and 3 are believed to be the result of permeability differences in the two cores. In addition to the permeability variations indicated in Table 15, which were determined prior to the initiation of these displacements, it is assumed that repeated CO_2 flooding exerts an appreciable effect on the permeabilities of these cores.

In displacements performed with oil P, the WFR and S_{OR} are slightly higher in Core 2 than the corresponding values reported for Core 3, and CO_2 BT occurs significantly later in Core 2. For displacements performed with the synthetic oil blend, P/A-P, the WFR is significantly lower in Core 2; while, the S_{OR} is notably higher. CO_2 BT again occurs later in Core 2. Economic restrictions and time limitations did not permit the execution of additional CO_2 floods with these oils in order to establish some sort of reproducibility among these parameters for the two cores involved. Runs 7 and 9 with oil P/A, however, were both performed in Core 2, and examination of the WFR, S_{OR} , and CO_2 BT data for both runs indicate that these results are in close agreement. It appears then that differences noted in these parameters for displacements with a given oil are, therefore, due to variations in the cores. While ROR are slightly higher from displacements performed in Core 2, sufficient reproducibility exists between the recoveries obtained with a particular oil, regardless of the core involved, so that recovery differences among the oils are considered to be functions of the synthetic oil chemistry and the displacement mechanism.

According to the visual observations performed during the tertiary CO_2 floods with the P/A oil, Runs 7 and 9 exhibit first-contact miscible (FCM) displacement mechanisms at 1300 psia and 100°F. The phase behavior observed during Runs 4 and 8 with the P oil and Runs 5 and 6 with the P/A-P oil indicate that miscibility is developed via the multiple-contact miscible (MCM) displacement mechanism at 1300 psia and 100°F. The visual observations are, thus, consistent with the P-X diagrams of these synthetic oils (Figures 14, 15 and 16). As expected, the highest residual oil recoveries, 92.0 and 94.4%, were obtained from the FCM displacements with oil P/A. Appreciable differences are noted, however, in the residual oil recoveries obtained from displacements with the P oil and the P/A-P oil. While CO_2 floods with both of these oils exhibit MCM displacement mechanisms, significantly higher recoveries were obtained with the P/A-P oil, 87.2 and 89.5%, as compared to the recoveries obtained with the P oil, 72.7 and 77.9.

To examine whether the improved recoveries obtained with the P/A-P oil were the result of compositional effects or variations in flood conformance, differences in mobility were considered. Once an oil bank has formed, the mobility ratio at the flood front is dominated by the viscosity differences between the oil and CO_2 . The viscosity of CO_2 at run conditions (0.0357 cp.; Michels et al., 1975) is significantly less than the viscosities of either synthetic oil (Table 18). However, the viscosity ratio for Oil P/A-P is slightly more favorable than that for Oil P. Comparing the FRT of CO_2 BT

Table 20
Results of Unsuccessful Tertiary Corefloods

Run No.	Core No.	Oil	Run Temperature (C°)	cc's CO ₂ * Injected At CO ₂ BT	cc's CO ₂ * Injected at GOR=30,000 SCF/STB	CO ₂ BT Fractional** Run Time (FRT)	% Recovery of Oil in Core From H ₂ O Flood (WFR)	SOR	% Recovery of Residual Oil From CO ₂ Flood (ROR)	Phase Behavior and Displacement Mechanism
1	3	P/A	40.0	210	683	0.31	33.2	0.320	86.5	Sight-glass blow-outs prevented visual observations.
2	3	P/A	37.0	184	639	0.29	28.5	0.285	89.5	Single oil phase observed throughout the run, indicating a FCM process.
3	3	P	38.0	236	744	0.32	36.6	0.322	81.8	Two phase flow of oil occurred at 0.53 FRT. Phase behavior and oil recovery indicate a MCH process.

* cc's of CO₂ injected were measured directly from the Ruska pump at room temperature and run pressure.

** FRT = $\frac{\text{cc's of CO}_2 \text{ injected at the point of interest}}{\text{cc's of CO}_2 \text{ injected at GOR} = 30,000 \text{ SCF/STB}}$

Table 21
Results of Successful Tertiary Corefloods

Run No.	Core No.	Oil	Run Temperature (C°)	cc's CO ₂ * Injected* At CO ₂ BT	cc's CO ₂ * Injected* at GOR=30,000 SCF/STB	CO ₂ BT Fractional** Run Time (FRT)	% Recovery of Oil in Core From H ₂ O Flood (WFR)	SOR	% Recovery of Residual Oil From CO ₂ Flood (ROR)	Phase Behavior and Displacement Mechanism
7	2	P/A	38.0	269	538	0.50	39.4	0.333	92.0	Single oil phase observed throughout the run indicating FCM process.
9	2	P/A	38.0	359	676	0.53	38.9	0.343	94.4	Single oil phase observed throughout the run indicating a FCM process.
4	3	P	38.0	184	578	0.32	34.2	0.343	72.7	Two phase flow of oil occurred at 0.53 FRT. Broad, ill-defined oil/oil interface. Phase behavior and oil recovery indicate a MCM process.
8	2	P	38.5	302	489	0.62	38.1	0.383	77.9	Two phase flow of oil occurred at 0.89 FRT. Phase behavior and oil recovery indicate a MCM process.
5	3	P/A-P	38.0	236	648	0.36	37.6	0.311	87.2	Two phase flow of oil occurred at 0.74 FRT. Phase behavior and oil recovery indicate a MCM process.
6	2	P/A-P	37.5	269	579	0.46	26.7	0.370	89.5	Two phase flow of oil occurred at 0.87 FRT. Phase behavior and oil recovery indicate a MCM process.

* cc's of CO₂ injected were measured directly from the Ruska pump at room temperature and run pressure.

** FRT = cc's of CO₂ injected at the point of interest

cc's of CO₂ injected at GOR = 30,000 SCF/STB

within a particular core for the two oils, it appears that CO₂ BT in Core 3 occurred at approximately the same FRT for both oils (Runs 4 and 5). However, comparing Run 8 (Oil P) and Run 6 (Oil P/A-P) performed in Core 2, CO₂ BT occurred significantly later in the displacement with oil P. This suggests that the increased recoveries obtained with the P/A-P oil are not the result of improved flood conformance.

Similarly, a comparison of the phase behavior observed during displacements within a particular core for runs involving both oils was performed. In Core 2, the two phase flow of oil is observed at approximately equivalent FRT's in Run 8 (P) and Run 6 (P/A-P). According to the phase observations noted for displacements in Core 3, however, two phase flow is observed at 0.53 FRT in Run 4 (P) and at 0.74 FRT in Run 5 (P/A-P). The phase behavior of the displacements performed in Core 3, therefore, suggests that miscibility is developed significantly earlier in the flood involving the P/A-P oil, Run 5. This analysis indicates that the improved recoveries obtained with the P/A-P oil are most likely the result of compositional effects.

The nature of these effects were further investigated by performing compositional analyses on synthetic oil samples obtained during the various CO₂ floods.

Compositional Analyses Performed for Corefloods Using Synthetic Oils

The results of the synthetic oil coreflood compositional analyses are presented in Tables 22-27 and Figures 19-24. Compositional analyses of samples obtained from the aforementioned unsuccessful displacements, Runs 1, 2 and 3, are presented in Tables 28-30. While data from unsuccessful displacements is not considered in the following discussion, it should be noted that all the results are in agreement with the ensuing conclusions.

Produced fluids obtained from the tertiary corefloods were collected at random intervals in 100 ml. graduated cylinders. Upon standing overnight, samples of the pooled fluids were procured for compositional analyses. Samples obtained in this manner are, therefore, representative of the collective production for a given period of time. This is particularly significant when attempting to determine the compositions of transition zone fluids, which typically exist for relatively brief intervals during these displacements.

Because the effluent samples were arbitrarily collected at random intervals, it is difficult to compare samples from one flood to those of another on a one to one basis. To facilitate the interpretation of results, the dimensionless time variable is again utilized to indicate at what point during each displacement a particular sample was procured. This dimensionless variable, referred to as the fractional run time (FRT), corresponds to the cc's of CO₂ injected at the time of sampling relative to the cc's of CO₂ injected when the producing GOR reached 30,000 SCF/STB. (The volumes of CO₂ injected were measured at room temperature and run pressure.)

$$FRT = \frac{\text{cc's of CO}_2 \text{ injected at the point of interest}}{\text{cc's of CO}_2 \text{ injected at GOR} = 30,000 \text{ SCF/STB}}$$

Table 22

Compositional Analyses of Samples from Run 7
(mole fractions)

Run No.: 1

$$\bar{S}_w = 0.67$$

Oil: P/A

$$S_{OR} = 0.33$$

System: Core 2

$$\% \text{ Recovery} = 92.0\%$$

Sample No.	Synthetic Oil	1	2	3	4	5
Observations		Two Phase Flow; Oil and Brine	Two Phase Flow; Brine and oil (CO ₂ BT)	Single Phase Flow; Oil	Single Phase Flow; Oil	Single Phase Flow; Oil
FRT		0.34	0.50	0.64	0.90	1.00
<u>Components</u>						
C ₅	0.20	0.20	0.20	0.11	0.05	0.03
C ₁₀	0.30	0.30	0.30	0.34	0.36	0.34
C ₁₀ '	0.20	0.20	0.20	0.22	0.23	0.24
C ₂₀ '	0.20	0.20	0.20	0.22	0.24	0.26
C ₃₀ '	<u>0.10</u>	<u>0.10</u>	<u>0.10</u>	<u>0.11</u>	<u>0.12</u>	<u>0.13</u>
	1.00	1.00	1.00	1.00	1.00	1.00

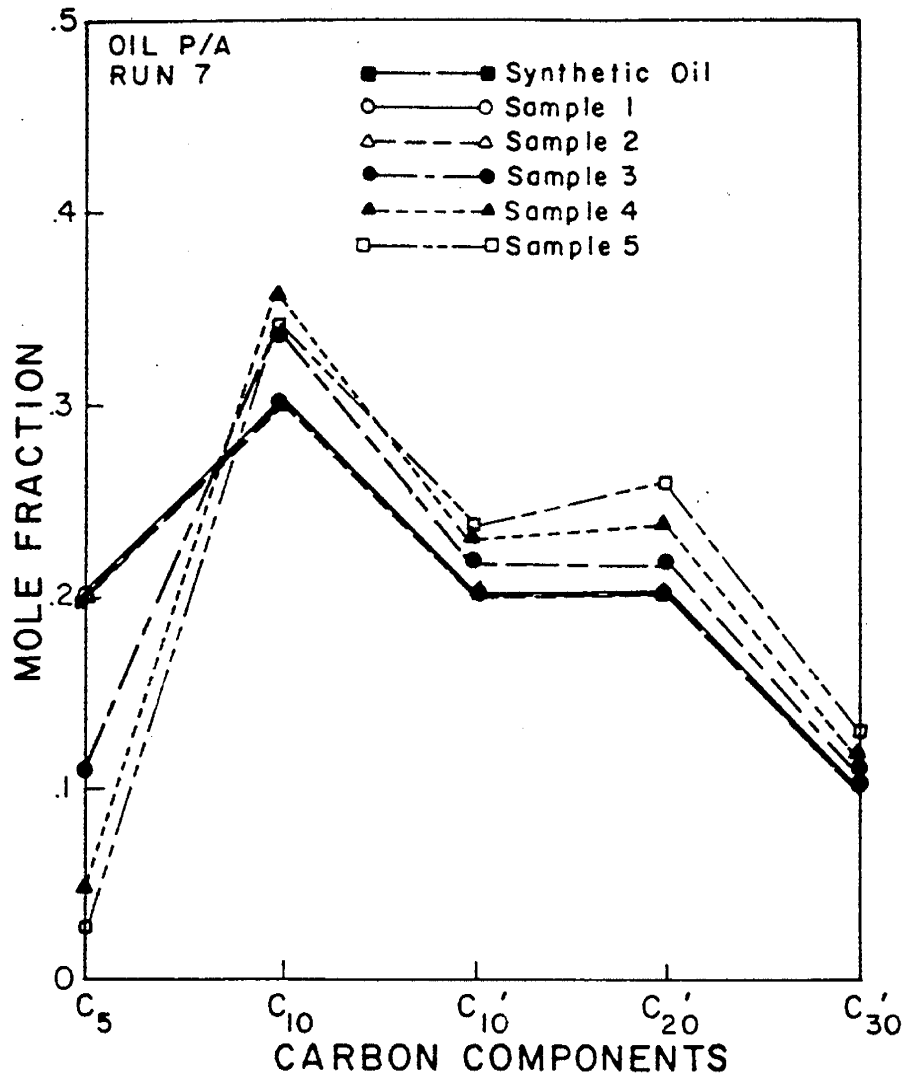


Figure 19. Compositional Analyses of Samples from Run 7

Table 23

Compositional Analyses of Samples from Run 9
(mole fractions)

Run No.: 9

$$\bar{S}_w = 0.66$$

Oil: P/A

$$S_{OR} = 0.34$$

System: Core 2

$$\% \text{ Recovery} = 94.4\%$$

Sample No.	Synthetic Oil	1	2	3	4
Observations		Two Phase Flow; Oil and Brine	Single Phase Flow; oil (CO ₂ BT)	Single Phase Flow; Oil	Single Phase Flow; Oil
FRT		0.39	0.53	0.75	0.95
<u>Components</u>					
C ₅	0.20	0.20	0.20	0.11	0.03
C ₁₀	0.30	0.30	0.30	0.34	0.35
C ₁₀ '	0.20	0.20	0.20	0.21	0.23
C ₂₀ '	0.20	0.20	0.20	0.23	0.25
C ₃₀ '	<u>0.10</u>	<u>0.10</u>	<u>0.10</u>	<u>0.11</u>	<u>0.14</u>
	1.00	1.00	1.00	1.00	1.00

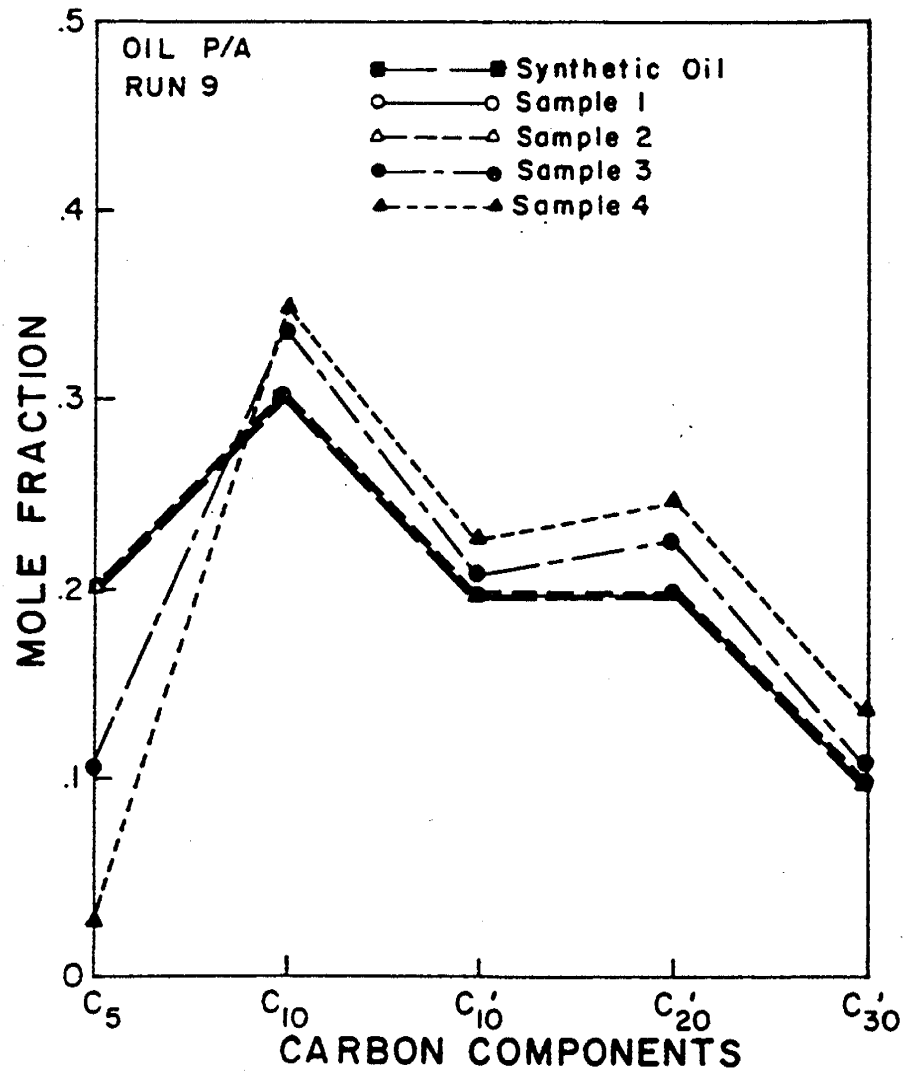


Figure 20. Compositional Analyses of Samples from Run 9

Table 24

Compositional Analyses of Samples from Run 4
(mole fractions)

Run No.: 4 $\bar{S}_w = 0.66$
 Oil: P $S_{OR} = 0.34$
 System: Core 3 % Recovery = 72.7%

Sample No.	Synthetic Oil	1	2	3	4	5
Observations		Two Phase Flow; Oil and Brine	Single Phase Flow; Oil (after CO ₂ BT)	Two Phase Flow; Oil	Two Phase Flow; Oil	Two Phase Flow; Oil
FRT		0.27	0.39	0.53	0.67	0.97
<u>Components</u>						
C ₅	0.20	0.18	0.08	0.05	0.04	0.01
C ₁₀	0.50	0.50	0.58	0.58	0.66	0.77
C ₂₀	0.20	0.21	0.23	0.23	0.20	0.16
C ₃₀	<u>0.10</u>	<u>0.11</u>	<u>0.11</u>	<u>0.14</u>	<u>0.10</u>	<u>0.06</u>
	1.00	1.00	1.00	1.00	1.00	1.00

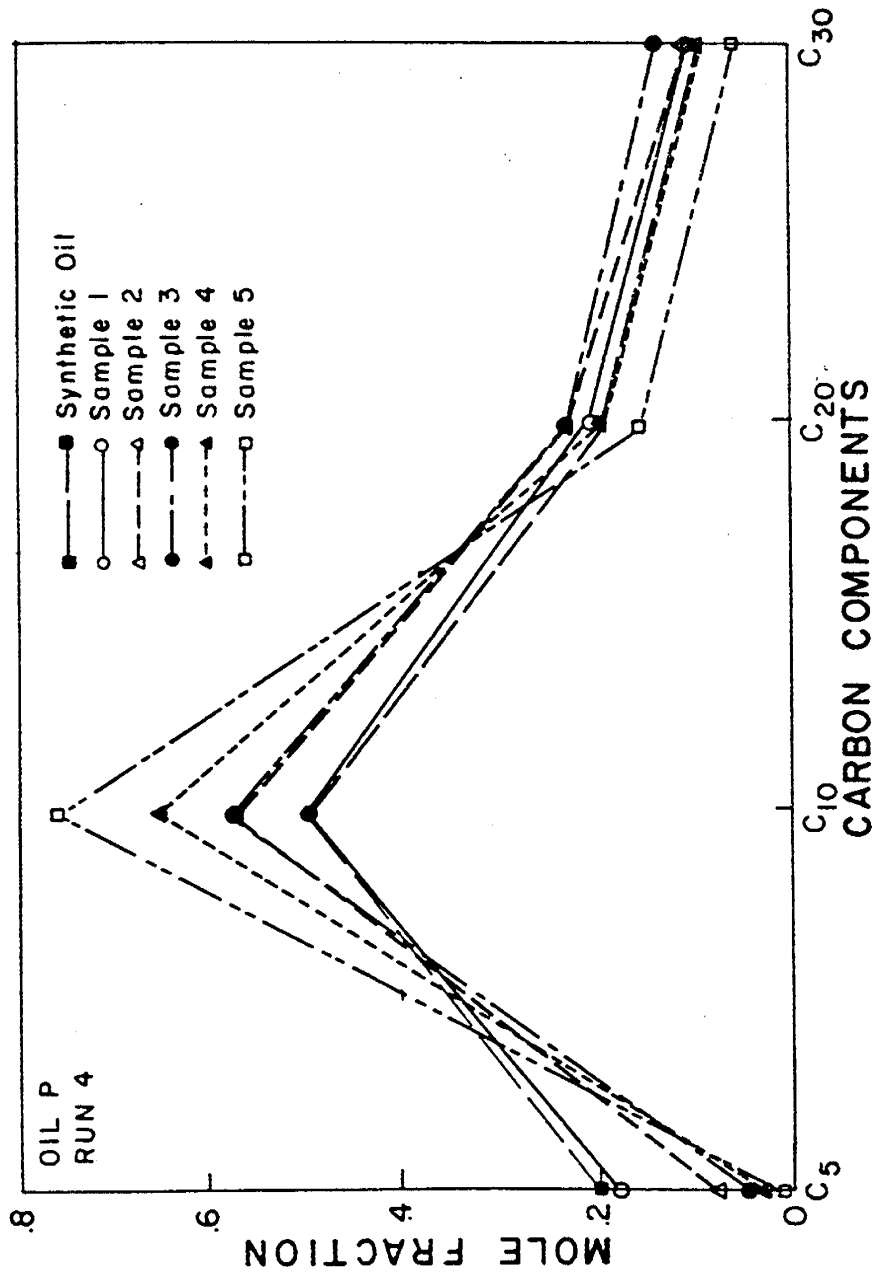


Figure 21. Compositional Analyses of Samples from Run 4

Table 25

Compositional Analyses of Samples from Run 8
(mole fractions)

Run No.: 8

$$\bar{S}_w = 0.62$$

Oil: P

$$S_{OR} = 0.38$$

System: Core 2

$$\% \text{ Recovery} = 77.9\%$$

Sample No.	Synthetic Oil	1	2	3	4
Observations		Single Phase Flow; Oil	Single Phase Flow; Oil	Two Phase Flow; Oil (after CO ₂ BT)	Single Phase Flow; Oil
FRT		0.42	0.59	0.94	1.00
<u>Components</u>					
C ₅	0.20	0.21	0.21	0.05	0.03
C ₁₀	0.50	0.51	0.51	0.45	0.61
C ₂₀	0.20	0.19	0.19	0.29	0.23
C ₃₀	<u>0.10</u>	<u>0.09</u>	<u>0.09</u>	<u>0.21</u>	<u>0.13</u>
	1.00	1.00	1.00	1.00	1.00

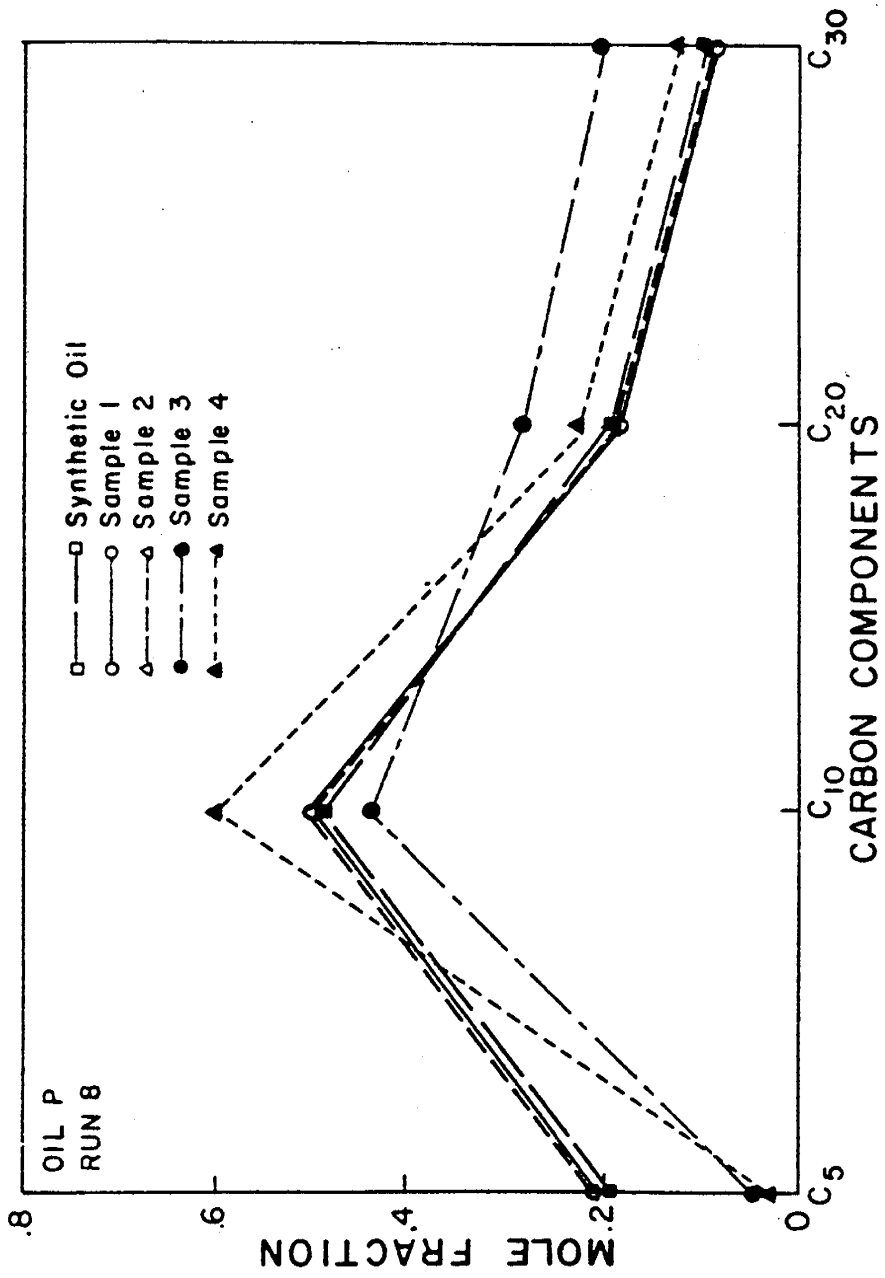


Figure 22. Compositional Analyses of Samples from Run 8

Table 26

Compositional Analyses of Samples from Run 5
(mole fractions)

Run No.: 5	$\bar{S}_w = 0.69$
Oil: P/A-P	$S_{OR} = 0.31$
System: Core 3	% Recovery = 87.2%

Sample No.	Synthetic Oil	1	2	3	4	5
Observations		Two Phase Flow; Oil and Brine	Two Phase Flow; Oil and Brine (CO ₂ BT)	Single Phase Flow; Oil	Single Phase Flow; Oil	Two Phase Flow; Oil
FRT		0.30	0.37	0.43	0.66	1.00
<u>Components</u>						
C ₅	0.20	0.18	0.19	0.11	0.06	0.05
C ₁₀	0.40	0.41	0.41	0.45	0.46	0.47
C ₁₀ '	0.10	0.11	0.10	0.11	0.12	0.12
C ₂₀ '	0.10	0.10	0.10	0.11	0.12	0.12
C ₃₀ '	0.05	0.05	0.05	0.06	0.05	0.05
C ₂₀	0.10	0.10	0.10	0.11	0.12	0.12
C ₃₀	<u>0.05</u>	<u>0.05</u>	<u>0.05</u>	<u>0.05</u>	<u>0.07</u>	<u>0.07</u>
	1.00	1.00	1.00	1.00	1.00	1.00

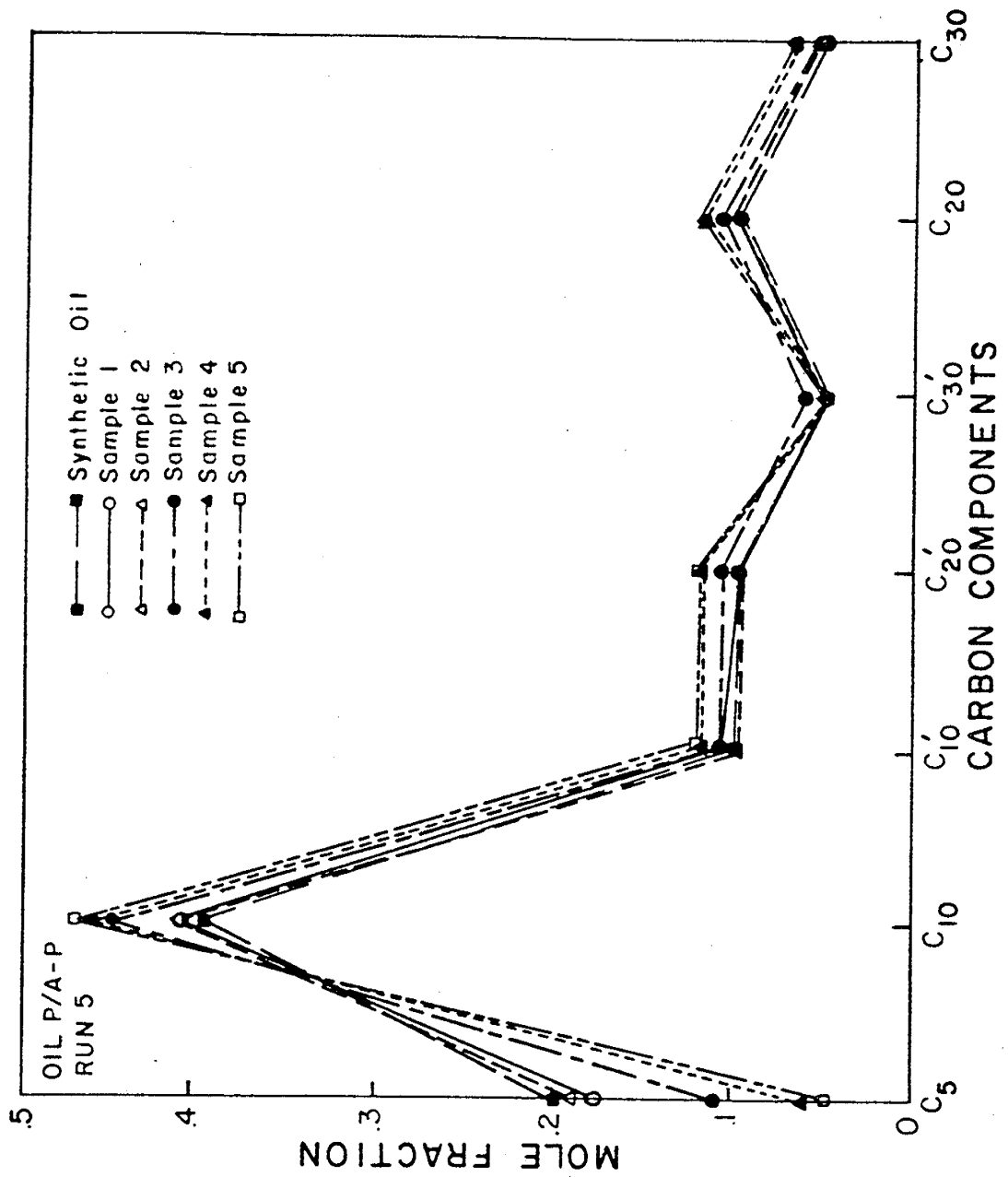


Figure 23. Compositional Analyses of Samples from Run 5

Table 27

Compositional Analyses of Samples from Run 6
(mole fractions)

Run No.: 6

$$\bar{S}_w = 0.63$$

Oil: P/A-P

$$S_{OR} = 0.37$$

System: Core 2

$$\% \text{ Recovery} = 89.5\%$$

Sample No.	Synthetic Oil	1	2	3	4	5
Observations		Two Phase Flow; Oil and Brine	Two Phase Flow; Oil and Brine	Two Phase Flow; Oil & Brine (after CO ₂ BT)	Two Phase Flow; Oil and Brine	Two Phase Flow; Oil
FRT		0.33	0.42	0.55	0.70	1.00
<u>Components</u>						
C ₅	0.20	0.19	0.19	0.12	0.10	0.04
C ₁₀	0.04	0.41	0.41	0.45	0.46	0.49
C ₁₀ '	0.10	0.11	0.11	0.12	0.11	0.13
C ₂₀ '	0.10	0.09	0.09	0.10	0.10	0.13
C ₃₀ '	0.05	0.05	0.05	0.05	0.05	0.07
C ₂₀	0.10	0.09	0.09	0.10	0.11	0.10
C ₃₀	<u>0.05</u>	<u>0.06</u>	<u>0.06</u>	<u>0.06</u>	<u>0.07</u>	<u>0.04</u>
	1.00	1.00	1.00	1.00	1.00	1.00

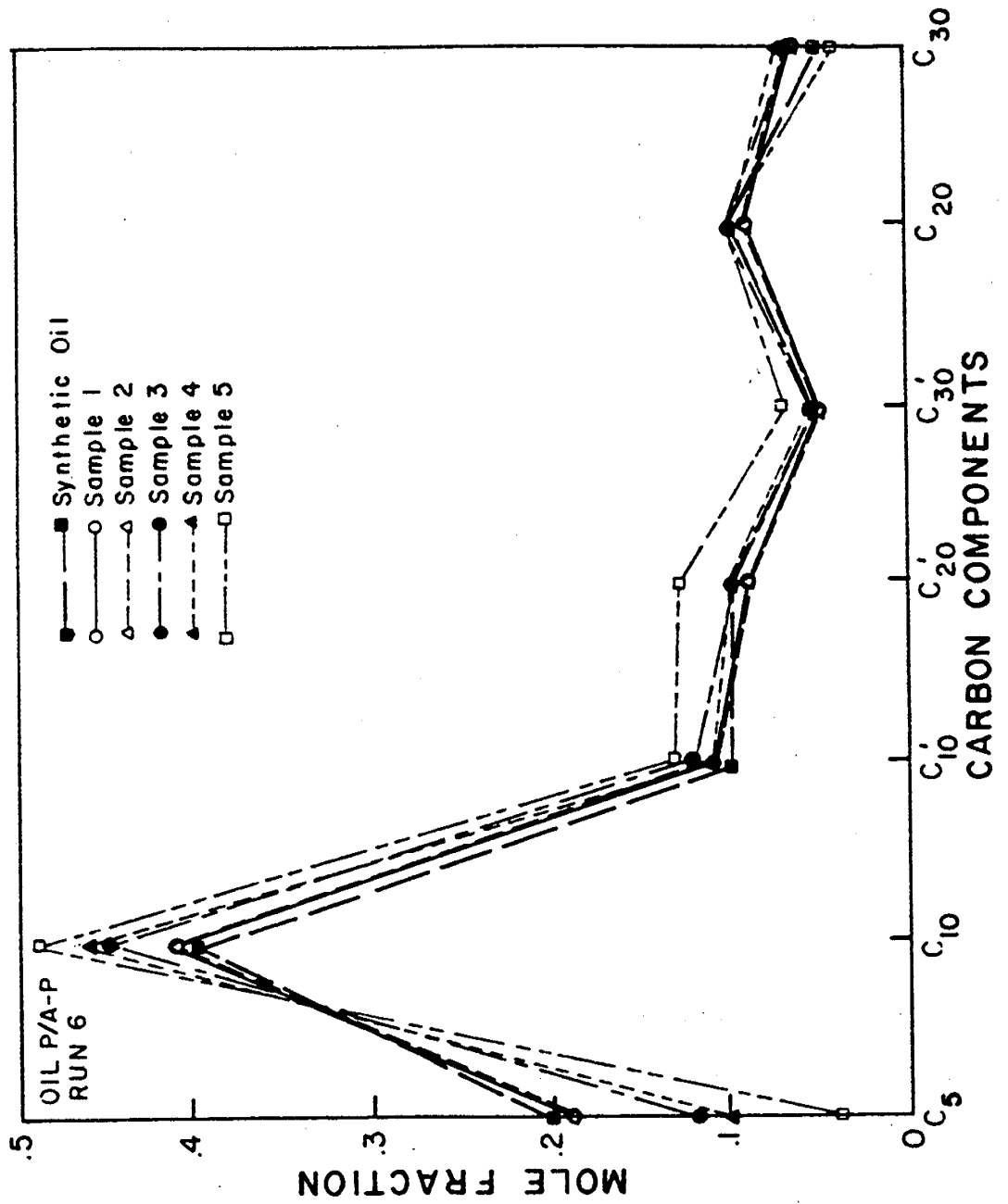


Figure 24. Compositional Analyses of Samples from Run 6

Table 28

Compositional Analyses of Samples from Run 1
(mole fractions)

Run No.: 1

$$\bar{S}_w = 0.68$$

Oil: P/A

$$S_{OR} = 0.32$$

System: Core 3

$$\% \text{ Recovery} = 86.4\%$$

Sample No.	Synthetic Oil	1	2	3	4	5
Observations		Two Phase Flow; Oil and Brine	Single Phase Flow; Oil (CO ₂ BT)	Single Phase Flow; Oil	*	*
FRT		0.23	0.31	0.52	0.87	0.99
<u>Components</u>						
C ₅	0.20	0.17	0.20	0.06	0.04	0.01
C ₁₀	0.30	0.31	0.30	0.35	0.36	0.35
C ₁₀ '	0.20	0.21	0.20	0.24	0.24	0.25
C ₂₀ '	0.20	0.21	0.20	0.24	0.24	0.26
C ₃₀ '	<u>0.10</u>	<u>0.10</u>	<u>0.10</u>	<u>0.11</u>	<u>0.12</u>	<u>0.13</u>
	1.00	1.00	1.00	1.00	1.00	1.00

* Site glass blow-out prevented further visual observations.

Table 29

Compositional Analyses of Samples from Run 2
(mole fractions)

Run No.: 2

$$\overline{S_w} = 0.72$$

Oil: P/A

$$S_{OR} = 0.28$$

System: Core 3

$$\% \text{ Recovery} = 89.5\%$$

Sample No.	Synthetic Oil	1	2	3
Observations		Single Phase Flow; Oil (after CO ₂ BT)	Single Phase Flow; Oil	Single Phase Flow; Oil
FRT		-0.52	0.71	0.98
<u>Components</u>				
C ₅	0.20	0.09	0.05	0.03
C ₁₀	0.30	0.33	0.34	0.36
C ₁₀ '	0.20	0.23	0.24	0.24
C ₂₀ '	0.20	0.23	0.24	0.24
C ₃₀ '	<u>0.10</u>	<u>0.12</u>	<u>0.13</u>	<u>0.13</u>
	1.00	1.00	1.00	1.00

Table 30

Compositional Analyses of Samples from Run 3
(mole fractions)

Run No.: 3

$$\bar{S}_w = 0.68$$

Oil: P

$$S_{OR} = 0.32$$

System: Core 3

$$\% \text{ Recovery} = 81.8\%$$

Sample No.	Synthetic Oil	1	2	3	4	5
Observations		Two Phase Flow; Oil and Brine	Two Phase Flow; Oil and Brine (CO ₂ BT)	Two Phase Flow; Oil	Two Phase Flow; Oil	Two Phase Flow; Oil
FRT		0.24	0.38	0.62	0.85	0.99
<u>Components</u>						
C ₅	0.20	0.16	0.11	0.06	0.04	0.01
C ₁₀	0.50	0.56	0.64	0.70	0.71	0.75
C ₂₀	0.20	0.17	0.16	0.16	0.17	0.17
C ₃₀	<u>0.10</u>	<u>0.11</u>	<u>0.09</u>	<u>0.08</u>	<u>0.08</u>	<u>0.07</u>
	1.00	1.00	1.00	1.00	1.00	1.00

For the most part, samples obtained in the early portions of each displacement, prior to CO₂ BT, represent the virgin synthetic oils. The following discussion, therefore, centers on the analyses of samples procured after CO₂ BT, which exhibit the most pronounced compositional changes.

According to Figure 14, tertiary CO₂ floods, Runs 7 and 9, with the paraffin/aromatic oil (P/A) exhibit a FCM mechanism at 1300 psia and 100°F. Analyses of samples obtained during Runs 7 and 9 should, therefore, indicate little or no compositional variation due to component partitioning. Significant decreases are observed, however, in the C₅ component with concomitant increases occurring in the other four components after CO₂ BT (Tables 22 and 23 and Figures 19 and 20). Because visual observations support the absence of transition zone fluids and confirm a FCM flood for oil P/A, the apparent decrease in C₅ is likely due to the greater volatility of this component. Previously performed flash analyses of PVT samples indicated that C₅ is preferentially swept into the wet test meter with CO₂. Loss of the C₅ constituent in this manner would also account for the observed increases in the mole fractions of the other four components. Compositional profiles of the three synthetic oils without the C₅ component are presented in Table 31. The profile for oil P/A is similar to the compositional analyses of samples obtained near the end of Runs 7 and 9. In summation, it appears that the observed compositional variations are the result of the increased volatility of C₅ and that no component partitioning occurred, consistent with a FCM mechanism for displacements with oil P/A.

In contrast to the Oil P/A results, tertiary core floods with the 100% paraffin oil (P) exhibit a MCM displacement mechanism at 1300 psia and 100°F (Figure 15). Compositional analyses of samples obtained during Runs 4 and 8 indicate similar, appreciable decreases in the C₅ component after CO₂ BT; however, different behavior is apparent for the three heavier components (Tables 24 and 25 and Figures 21 and 22). If the compositional variations noted after CO₂ BT were solely the result of losses occurring in the C₅ component (as in Runs 7 and 9), then compositional profiles should indicate concomitant increases in the mole fractions of the other three components (Table 31).

In Run 4 (Core 3) dramatic increases are exhibited in the C₁₀ component after CO₂ BT. Slight increases are observed just after BT in the heavier components, C₂₀ and C₃₀, followed by decreases in these constituents near the end of the flood. In addition visual observations performed during this displacement indicate the appearance of two oil phases at approximately 0.53 FRT (Table 21). These results suggest that component partitioning was occurring and that the C₂₀ and C₃₀ constituents were being selectively left behind in the developing transition zone of Run 4.

This same observation is not readily apparent from the compositional analyses of samples from Run 8. The compositional profile of samples obtained after CO₂ BT indicate significant decreases in C₅. Initially a slight decrease is noted in C₁₀ after CO₂ BT, followed by a notable increase later in the displacement. Increases are noted in the mole fractions of the heavier components, C₂₀ and C₃₀, just after CO₂ BT, followed by slight decreases in these constituents somewhat later in the run. Visual observations obtained during Run 8 (Core 2) indicate the appearance of two oil phases at approximately 0.89 FRT, noticeably later than the occurrence of two oil phase in Run

Table 31

Compositional Profile of Synthetic Oils Without C₅

Synthetic Oils:	P/A	P	P/A-P
<u>Components</u>	<u>mole %</u>	<u>mole %</u>	<u>mole %</u>
C ₁₀	37	65	50
C ₁₀ '	25		12
C ₂₀ '	25		12
C ₃₀ '	13		7
C ₂₀		22	12
C ₃₀		13	7

4 (Table 21). This discrepancy, attributable to variations in the permeabilities of Cores 2 and 3, may account for differences noted in the compositional analyses of samples obtained after CO₂ BT in Runs 4 and 8. In addition, the sampling technique employed may have diluted the transition zone fluids enough to obscure the actual compositional profiles.

According to Figure 16 and visual observations, CO₂ displacements of oil P/A-P at 1300 psia and 100°F exhibit a MCM mechanism. In Runs 5 and 6, compositional analyses of samples obtained after CO₂ BT again indicate continuous decreases in the C₅ component with appreciable increases occurring in the C₁₀ component as the floods progress (Tables 26 and 27 and Figures 23 and 24). Slight increases are also noted in the other components after CO₂ BT in Run 5 (Core 3), except for C₃₀ which remains fairly constant. In Run 6 (Core 2), slight increases are observed in components C₁₀, C₂₀, and C₃₀ after CO₂ BT; whereas, the mole fractions of C₂₀ and C₃₀ remain relatively unchanged.

While these compositional variations may appear to be the result of losses in the volatile C₅ constituent, visual observations made during these displacements indicate the appearance of two oil phases at 0.74 FRT in Run 5 and 0.87 FRT in Run 6. The observed phase behavior, therefore, confirms the occurrence of actual component transfer between phases. Apparent differences in the compositional profiles of samples obtained from Runs 5 and 6 are again believed to be the result of the sampling technique and/or the permeability variations in the cores, as evidenced by the later CO₂ BT and occurrence of two oil phases observed in Core 2 (Table 21).

The compositional changes occurring in Run 5 with oil P/A-P suggest that the transition zone fluids developed during this displacement are richer in the heavier components, C₂₀ and C₃₀, than the corresponding transition zone fluids of Run 4 with oil P. This observation tends to support the hypothesis of Monger and Khakoo (1982) that increasing crude oil aromaticity improves hydrocarbon extraction into a CO₂-rich phase. Correspondingly, increased oil recoveries obtained from displacements with oil P/A-P as compared to oil P seem to correlate with the improved recovery of the heavier components, C₂₀ and C₃₀.

Vertical Coreflood Experimental Results

The experimental studies planned call for four series of CO₂ corefloods using reservoir oil from the Timbalier Bay field in La Fourche Parish, Louisiana at the reservoir temperature of 206°F. For all the displacements, 100% CO₂ will be used as the injection fluid. Tertiary flood conditions will be addressed because the reservoir has experienced a strong water drive. Two series of core displacements will use dead oil, and two will use reconstituted live oil. Gravity stable versus non gravity stable flood rates will be examined for both oil types to determine whether the reservoir's dip should be used to advantage to improve sweep out and oil recovery. Compositional profiles of the produced fluids and phase properties compiled from supportive PVT studies will be used to evaluate existing critical velocity equations.

A series of sandpack displacements were performed to determine the MMP at 200°F and to screen for solid phase formation. Oil recovery results and sight glass observations suggest an MMP of about 3,500 psig at 200°F. No solid phase was visible during the floods. Generally, the phase behavior observed

was initial production of black virgin oil, followed by a transition zone of wine-red colored oil changing to clear light-amber colored liquid. Below the MMP, virgin oil was still produced after a less defined transition zone.

Progress achieved to date has focussed on dead oil displacements using non-gravity stable displacement rates. The results of five corefloods are summarized in Tables 32 and 33. This data is considered to be preliminary.

The data in Table 33 suggest an initial piston-like displacement of oil with CO_2 , followed by a zone in which the CO_2 and oil become increasingly miscible with continuing contact. After this transition zone has passed, most of the oil in the swept zone has been displaced, and the displacement mechanism is again piston like, with pure injection fluid pushing the transition zone.

CONCLUSIONS

1. Tertiary CO_2 corefloods using synthetic oils exhibit improved oil recoveries with increasing aromatic content. Compositional analyses of effluent samples show that the improved oil recoveries correlate with enhanced recovery of the heavier paraffinic components, C_{20} and C_{30} . Visual observations of the phase behavior occurring during these displacements also suggest that the presence of aromatics enhances the CO_2 extraction mechanism, thereby accelerating the development of miscibility in the multiple-contact process.
2. The effect of oil aromaticity shown by the coreflood results typifies the well-known relationship between phase behavior and MCM displacement efficiency, and establishes that oil chemistry effects can compete with the numerous other variables that control CO_2 flood performance.
3. Results of gravity stable tertiary corefloods using 100% CO_2 as injection fluid and Timblier Bay reservoir oil are too preliminary to formulate conclusions.

Table 32

Results of Vertical Corefloods

Run No.	Core No.	Press. psi	Temp. F°	Rec. after H ₂ O flood, cc/%	Rec. after CO ₂ flood, cc/%
1	1	3500	200	139, 31% 001P	228, 51% 001P 73% 01P
*2	1	4000	200	205, 48% 001P	225, 53% 001P 103% 01P
3	1	3500	200	137, 30% 001P	234, 52% 001P 75% 01P
4	1	4000	200	162, 34% 001P	272, 58% 001P 75% 01P
5	2	3000	200	no water flood	272, 68% 001P

* Indicated need for core cleaning.

Table 33

Phase Behavior Observations During Vertical Corefloods

<u>Run No.</u>	<u>CO₂ displaced, fraction of pore volume</u>	<u>Effluent Observation</u>
1	0	clear; single liquid phase (brine)
	20	wine red; brown liquids
	75	clear; single phase fluid
2	0	clear; single liquid phase (brine)
	31	wine red; brown liquids
	54	clear; single phase fluid
3	0	clear; single liquid phase (brine)
	37	wine red; brown liquids
	51	clear; single phase fluid
4	0	clear; single liquid phase (brine)
	34	wine red; brown liquids
	57	clear; single phase fluid
5	0	clear; single liquid phase (brine)
	29	wine red; brown liquids
	74	clear; single phase fluid

BIBLIOGRAPHY

- Blackwell, R. J., Rayne, J. R., and Terry, W. M. (1959) "Factors Influencing the Efficiencies of Miscible Displacements," Trans. AIME (1959), 216, 1.
- Cardenas, R. L., Alston, R. B., Nute, A. J., and Kokolis, G. P. (1984) "Laboratory Design of a Gravity Stable, Miscible CO₂ Process," J. Pet. Tech. (January, 1984) 111.
- Dumoré, J. M. (1964) "Stability Considerations in Downward Miscible Displacement," Soc. Pet. Eng. J. 4 (December, 1964) 356.
- Gardner, J. W., Orr, F. M., and Patel, P. D. (1981) "The Effect of Phase Behavior on CO₂ Flood Displacement Efficiency," J. Pet. Tech. 33 (November, 1981) 2067.
- Gardner, J. W. and Ypma, J. G. J. (1984) "An Investigation of Phase Behavior-Macroscopic Bypassing Interaction in CO₂ Flooding," Soc. Pet. Eng. J. 24 (October, 1984) 508.
- Hill, S. (1949) "Channelling in Packed Columns," Chem. Eng. Sci. (1949) 1, 247.
- Holm, L. W. (1959) "Carbon Dioxide Solvent Flooding for Increased Oil Recovery," Petroleum Transactions, AIME (1959) 216, 225.
- Holm, L. W. and Josendal, V. A. (1974) "Mechanisms of Oil Displacement by Carbon Dioxide," J. Pet. Tech. (December, 1974) 1427.
- Holm, L. W. and Josendal, V. A. (1980) "Effect of Oil Composition on Miscible-Type Displacement by Carbon Dioxide," J. Pet. Tech. (February, 1982) 87; "Discussion of Determination and Prediction of CO₂ Minimum Miscibility Pressures," J. Pet. Tech. (May, 1980) 870.
- Huang, E. T. S. and Tracht, J. H. (1974) "The Displacement of Residual Oil by Carbon Dioxide," SPE 4735, presented at the SPE 3rd Symposium on Improved Oil Recovery, Tulsa, April, 1974.
- Lacy, J. W., Draper, A. L., and Binder, G. G., Jr. (1958) "Miscible Fluid Displacements in Porous Media," Trans. AIME (1958) 231, 76.
- Leach, M. P. and Yellig, W. F. (1979) "Compositional Model Studies: CO₂ - Oil Displacement Mechanisms," SPE 8368, presented at 5th Annual Fall Technical Conference and Exhibition of the Society of Petroleum Engineers of AIME, Las Vegas, Sept. 23-26, 1979.
- Metcalfe, R. S. and Yarborough, L. (1979) "The Effect of Phase Equilibria on the CO₂ Displacement Mechanism," Soc. Pet. Eng. J. 19 (August, 1979) 242.
- Michels, A., Botzen, A., and Schwerman, W. (1975) "The Viscosity of Carbon Dioxide Between 0°C and 75°C at Pressures up to 2000 Atmospheres," Physica 23 (1975) 95.

- Monger, T. G. and Khakoo, A. (1981) "The Phase Behavior of CO₂ - Appalachian Oil Systems," SPE 10269, presented at the 56th Annual Fall Technical Conference and Exhibition, San Antonio, Oct. 5-7, 1981.
- Monger, T. G. and McMullan, J. H. (1983) "Investigations of Enhanced Oil Recovery Through Use of Carbon Dioxide," Report DOE/BC/10344-8 Second Annual Report for U. S. DOE Contract DE-AS19-80BC 10344 (August, 1983).
- Monger, T. G. (1985) "Investigations of Enhanced Oil Recovery Through Use of Carbon Dioxide," Report DOE/BC/10344-15 Final Report for U.S. DOE Contract DE-AS19-80BC10344, Volume I.
- Orr, F. M., Jr., Yu, A. D., and Lien, C. L. (1981) "Phase Behavior of CO₂ and Crude Oil in Low Temperature Reservoirs," Soc. Pet. Eng. J. 21 (August, 1981) 480.
- Orr, F. M., Silva, M. K., and Lien, C. L. (1983) "Equilibrium Phase Compositions of CO₂ - Crude Oil Mixtures-Part I: Comparison of Continuous Multiple Contact and Slim Tube Displacement Tests," Soc. Pet. Eng. J. 23 (April, 1983) 272; "Equilibrium Phase Compositions of CO₂ - Hydrocarbon Mixtures-Part II: Measurement by a Continuous Multiple Contact Experiment," Soc. Pet. Eng. J. 23 (April, 1983) 281.
- Palmer, F. S., Nute, A. J., and Peterson, R. L. (1984) "Implementation of a Gravity Stable, Miscible CO₂ Flood in the 8000-Foot Sand, Bay St. Elaine Field," J. Pet. Tech. (January, 1984) 101.
- Perry, G. E. (1982) "Weeks Island 'S' Sand Reservoir B Gravity Stable Miscible CO₂ Displacement, Iberia Parish, Louisiana," SPE/DOE 10695, presented at the Third SPE/DOE Symposium on EOR, Tulsa, April 4-7, 1982.
- Rathmell, J. J., Stalkup, F. I., and Hassinger, R. C. (1971) "A Laboratory Investigation of Miscible Displacement by Carbon Dioxide," SPE 3483, presented at 46th Annual SPE Fall Meeting, New Orleans, Oct. 3-6, 1971.
- Slobod, R. L. and Howlett, W. E. (1964) "The Effect of Gravity Segregation in Laboratory Studies of Miscible Displacements in Vertical Unconsolidated Porous Media," Trans. AIME (1964) 231, 1.
- Stalkup, F. I. (1983) "Miscible Displacement," Monograph Series 8, Society of Petroleum Engineers of AIME, Dallas, 1983.
- Whitehead, W. R., et al. (1981) "Investigations of Enhanced Oil Recovery Through Use of Carbon Dioxide," Report DOE/BC/10344-4 First Annual Report for U.S. DOE Contract DE-AS19-80BC10344 (July, 1982).

